THE SELECTIVE OSCILLATION OF THE CARBON DIOXIDE LASER

A Thesis

Presented in Partial Fulfillment of the Requirements
for the Degree Master of Science

by

John Thomas White, B.S.

The Ohio State University
1967

Approved by

Frederick P. Dickey
Adviser
Department of Physics

ACKNOWLEDGMENTS

The author would like to express his appreciation to his adviser, Dr. F. P. Dickey, for his guidance and support throughout the experimental work and the writing of this thesis. Furthermore, the author would like to thank Mr. H. E. Scott for his aid in the design of apparatus and his helpful suggestions pertaining to the experiment in general.

TABLE OF CONTENTS

LIST OF TABLES

LIST OF ILLUSTRATIONS

I. INTRODUCTION

During the early part of this century electromagnetic radiation was known to interact with matter, essentially electrons, atoms and molecules, by two processes -- spontaneous emission and absorption. Then in 1916 Albert Einstein (1) concluded on the basis of thermodynamic considerations that a third process exists, stimulated emission. These conclusions were quantitatively formulated in terms of transition rates of the matter units between energy levels. Given for example levels denoted 1 and 2 characterized by energies E_1 and E_2, where $E_2 > E_1$, the probability of a downward transition between the levels accompanied by a radiative emission in a radiation field of density $u(\nu)$ is

$$P_{21} = A_{21} + u(\nu) B_{21}. \tag{1.1}$$

Similarly, for an upward transition

$$P_{12} = u(\nu) B_{12}, \tag{1.2}$$

where A_{21}, B_{21}, and B_{12} are called the Einstein coefficients and characterize spontaneous emission, induced emission, and absorption respectively. They are related as follows:

$$A_{21} = (8\pi h\nu^3/c^3) B_{21}, \tag{1.3}$$

$$g_1 B_{12} = g_2 B_{21}. \tag{1.4}$$

The parameters g_1 and g_2 are the multiplicities of the indicated levels, h is Planck's constant, and c is the speed of light in the medium. Now Lambert's law for the intensity variance of a plane electromagnetic wave traveling in a homogeneous medium

$$dI_\nu / I_\nu = -k_\nu dz, \tag{1.5}$$

leads to an equation giving the intensity I_ν as a function of position z,

$$I_\nu = Io\ e^{-k_\nu z}, \tag{1.6}$$

where k_ν is termed the coefficient of absorption and the electromagnetic wave propagates in the positive z direction. It is apparent from equation (1.6) that if k_ν is positive the intensity decreases as the wave travels, that is a net energy absorption takes place in the medium.

In the early 1920's a relation was obtained by Füchtbauer and Ladenburg linking the coefficient of absorption k_ν with the Einstein coefficients. This relation leads (2) to the Füchtbauer-Ladenburg formula:

$$\int k_\nu d\nu = h\nu/c\ B_{12}N_1 \left[1 - (g_1/g_2)(N_2/N_1)\right]. \tag{1.7}$$

Here N_1 and N_2 are the number of matter units in the indicated states. Now for matter in thermodynamic equilibrium at temperature T the populations of energy states are governed by Boltzmann's law

$$(g_1/g_2)(N_2/N_1) = e^{-(E_2 - E_1)/KT}, \tag{1.8}$$

where K is Boltzmann's constant. Since $E_2 > E_1$, it follows from equation (1.8) that the second term in brackets in equation (1.7) is always less than one in the equilibrium situation, and that the integral on the left

hand side of equation (1.7) is positive. The implication of this result may be extended to the general case, and the statement can be made that when an electromagnetic wave propagates through a medium in thermodynamic equilibrium the net result of the interaction is an absorption of energy from the radiation field by the material of the medium. If, however, a non-equilibrium situation is established wherein

$$\frac{N_2}{g_2} > \frac{N_1}{g_1} , \tag{1.9}$$

the integral in equation (1.7) becomes negative, the direction of net energy transfer is reversed, and the radiation is amplified. Equation (1.9) quantitatively defines the situation whose establishment is known as a population inversion.

The period between the early 1920's and 1954 witnessed a number of attempts by various individuals to treat theoretically and experimentally the problem of maintaining a population inversion and constructing a radiation amplifier. Then in July of 1954 Townes and his students (3) published a paper announcing the successful construction and operation of a microwave amplifier, the first maser. The population inversion was accomplished by physically separating components of a molecular beam (NH_3) according to whether the molecules resided in an upper or lower energy state. It is an experimental fact that radiation produced through stimulated emission is coherent with the radiation inducing the emission. Townes found his maser produced radiation which was highly

directional and maintained extremely narrow line-widths. This experimental success stimulated activity in the field of quantum electronics and shortly a number of different masers were developed.

The common goal of most researchers engaged in this work was to extend maser action to the optical or infrared regions. The development of the maser preceded the laser probably for two reasons. First, a large amount of experimental work had been done during the war with microwaves and corresponding technology was at hand. Second, the typical microwave frequency is comparatively low. Spontaneous emission, which as indicated in equation (1.3) is dependent upon ν^3, has a minimal effect in this case and can often be ignored in obtaining a population inversion. The laser, while similar in basic theory, presented quite different problems in development, notably in design of the cavity of oscillation and the methods by which the populations of laser states might be inverted. Many of the problems associated with the construction were enumerated analytically in an "historic" article by Schawlow and Townes (3) published in 1958. Then in 1960 T. H. Maiman (4) reported successfully obtaining laser action in ruby. Shortly thereafter A. Javan (5) reported operation of the first gas laser, the helium-neon. The era of the laser was at hand. In the intervening years until the present, laser action has been obtained in diverse media including solids, liquids, glasses, gases, and semi-conductors. The basic theory and characteristics of lasers are by this time well known, and

no attempt will be made here to cover the subject. To the uninformed reader numerous papers and texts dealing with the subject could be recommended, of which references (2) and (6) are examples.

In 1964 C. K. N. Patel (7) reported continuous-wave (cw) laser action on a number of P-branch transitions in the $00^{o}1$-$10^{o}0$ and $00^{o}1$-$02^{o}0$ rotation-vibration bands of CO_2. The lasing medium was pure CO_2 excited by a dc discharge in the gas itself, and cw output power was measured on the strongest transition to be about one milliwatt. Then in 1965 Patel (8) reported construction of a "CW High Power N_2-CO_2 Laser" with an output of 11.9 watts from two transitions and an efficiency of about 3%, extremely high for a gas laser. It was hypothesized that vibrational energy transfer was taking place from the $v = 1$ level of N_2 to the upper laser level of CO_2. Later refinements, including the addition of helium (9), soon pushed output powers above 100 watts and efficiencies well over 6%.

In all of these experiments the transitions observed were in the P-branch alone and limited to certain J values involving comparatively high gain. In 1966 G. Moeller and J. D. Rigden (9) reported observation of R-branch transitions and many P-branch transitions previously not seen. This was done by employing a diffraction grating as a wavelength discriminating device at one end of the cavity of oscillation.

This thesis is concerned with the construction of a CO_2-N_2 laser excited by a continuous ac discharge in the medium, and the selective

oscillation thereof employing the method of Moeller and Rigden. The ability of the method to produce laser action yielding spectral lines not found in the output of the conventional CO_2 laser, and to do so selectively, is given theoretical support and experimental verification. Both the method and the analysis are general enough to be extended to all lasers employing linear polyatomic or diatomic molecules as the active medium.

II. THEORY

A. CO_2 Symmetries and Selection Rules

The carbon dioxide molecule is linear, and the equilibrium position of the carbon atom is symmetrically situated between those of the two oxygen atoms. The ground state oxygen nucleus has spin zero, and this is the case for the oxygen components of the carbon dioxide molecule involved in rotation-vibration transitions. It has been shown (10) that these conditions require that the antisymmetric rotation levels be missing entirely from the possible levels of excitation. This means that for Σ_g^+ electronic states the odd J rotational levels are absent, while for Σ_u^+ it is the even J levels which are missing. Here J is of course the rotational quantum number and the sigma symbolism used is standard electronic band notation. To a good approximation the selection rules governing transitions by means of radiative dipole emission or absorption for the cases of pure vibration and pure rotation are not altered by the interaction of rotational and vibrational states. The pertinent rules for linear molecules are given by Herzberg (10) as follows:

Vibrational component selection rules (2.1)

$$\ell = 0, \pm 1; \qquad \Sigma^+ \not\leftrightarrow \Sigma^-;$$

$$g \not\leftrightarrow g; \qquad u \not\leftrightarrow u.$$

Rotational component selection rules (2.2)

$$\Delta J = 0, \pm 1; \quad (J = 0 \not\longleftrightarrow J = 0);$$

$$+ \longleftrightarrow - ; \qquad s \not\longleftrightarrow a \quad .$$

Furthermore when $\ell = 0$ in both the upper and lower state (Σ-Σ transitions), $\Delta J = 0$ is excluded. Hence in Σ-Σ transitions the P-branch ($\Delta J = -1$) and the R-branch ($\Delta J = +1$) may be present, but the Q-branch ($\Delta J = 0$) is entirely absent. It should be noted here that these rules are strongly obeyed as dipole radiation is the predominant element in radiative transitions, however effects of non-linear forces and mechanical anharmonicities within the molecule frequently give rise to forbidden transitions, usually of comparatively weak intensities.

B. Inversion of Laser States

It has been mentioned earlier that high intensity laser output is observed, on the $00^{o}1$-$10^{o}0$ and $00^{o}1$-$02^{o}0$ bands of CO_2, from the CO_2-N_2 laser. These transitions are allowed under selection rules (2.1) and (2.2). Patel (8) postulated that an efficient transfer of vibrational energy between the $v = 1$ level of N_2 and the $00^{o}1$ level of CO_2 is the main mechanism for populating the upper laser state. In the original experiment N_2 was energetically excited before mixing with the CO_2 and entering the laser cavity, indicating other excitation mechanisms such as by electron impact directly with CO_2 are secondary.

Later investigations lead to the more efficient method of exciting the plasma in the cavity after mixing, since, contrary to original fears, the population inversion in CO_2 is not upset by the discharge.

Figure one is taken from Patel (11) and shows the relative positioning of the low-lying vibrational energy levels of CO_2 and N_2. It has been found (12) that a low-pressure discharge is highly effective for the excitation of N_2 to vibrational levels of the ground electronic state. Sobolev and Sokovikov (13) have submitted an analysis in which they take into account the conditions present in the CO_2 laser, and they contend the main process for exciting the N_2 molecule is direct electron excitation. However, other mechanisms such as atomic recombination and cascade processes are present and may be significant. The N_2 molecule, being homonuclear and diatomic, has no permanent dipole moment and thus cannot decay through radiative emission. Deactivation takes place by means of collisions with the walls of the container or other molecules and these processes are reported to be slow (14). A lifetime for the $v = 1$ state of 100 milliseconds has been obtained by Morgen and Schiff (15), and Dressler (12) has estimated that about ten to thirty percent of the molecules in a discharge will be in the $v = 1$ state. Referring again to figure one, it is seen there is excellent energy agreement between the $00^{o}1$ level of CO_2 and the $v = 1$ level of N_2, i.e. $\Delta E \approx 18\,cm^{-1}$. Furthermore, the distributions of rotational levels, which are superimposed upon the upper CO_2 laser level and the vibrationally excited N_2

Figure One

Pertinent energy levels of CO_2 and N_2 as given by Patel (11), indicating the mechanism for upper laser state population. The symbols (M) and (V.S.) refer to relative strengths of absorption bands and stand for "medium" and "very strong" respectively.

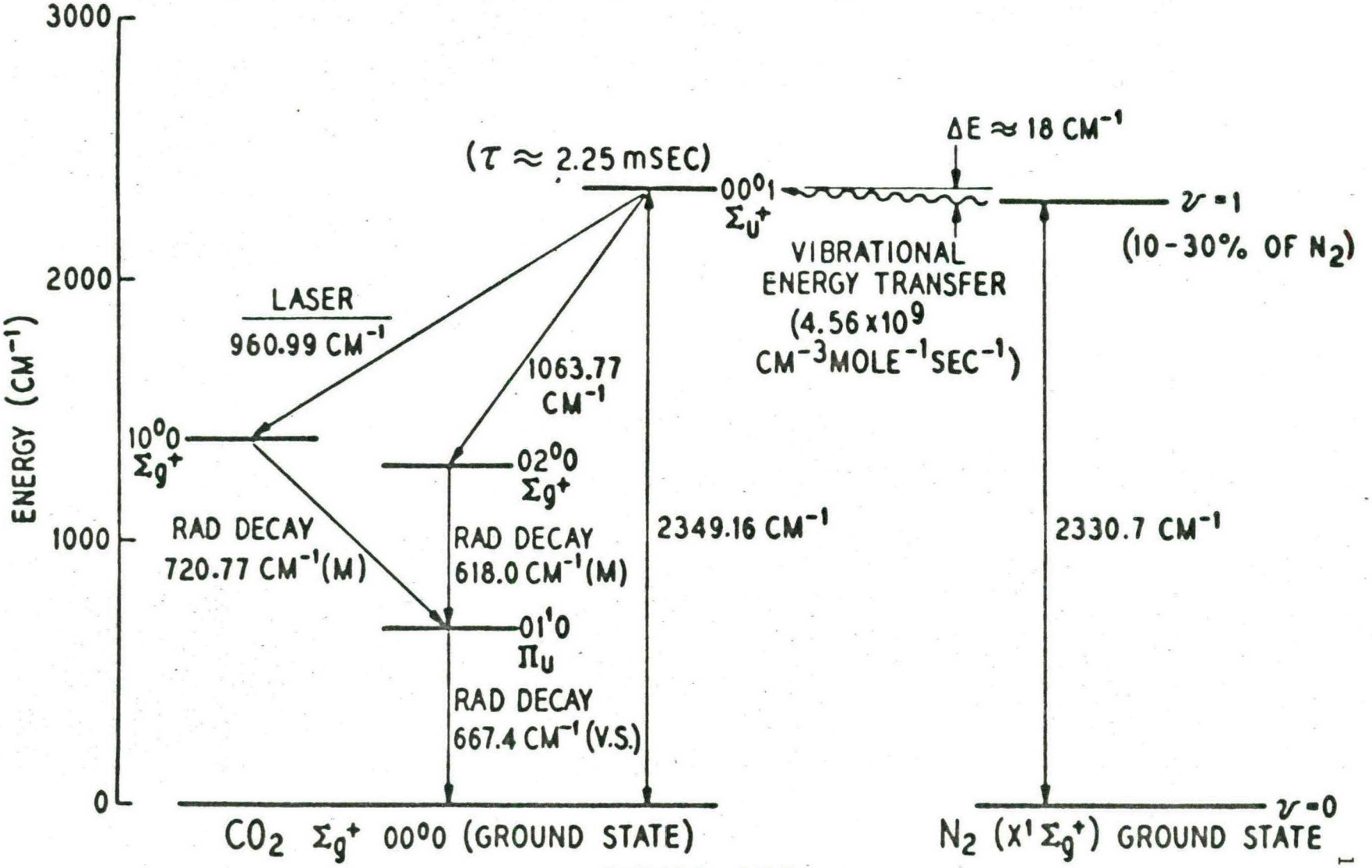
3000
2000
1000
0
ENERGY (CM⁻¹)
(τ ≈ 2.25 mSEC)
00⁰1
Σu⁺
ΔE ≈ 18 CM⁻¹
v = 1
(10-30% OF N2)
VIBRATIONAL
ENERGY TRANSFER
(4.56 x 10⁹
CM⁻³MOLE⁻¹SEC⁻¹)
LASER
960.99 CM⁻¹
1063.77
CM⁻¹
10⁰0
Σg⁺
02⁰0
Σg⁺
RAD DECAY
720.77 CM⁻¹(M)
RAD DECAY
618.0 CM⁻¹(M)
2349.16 CM⁻¹
2330.7 CM⁻¹
01¹0
Πu
RAD DECAY
667.4 CM⁻¹ (V.S.)
v = 0
CO2 Σg⁺ 00⁰0 (GROUND STATE)
N2 (X¹Σg⁺) GROUND STATE

FIGURE ONE

molecule, bring the energy states into even closer coincidence. The average thermal energy of the molecules (KT) at room temperature is 210^{-1}, more than a factor of ten greater than the average energy discrepancy. The possibility of strong quenching of N_2 (v = 1) by CO_2 is indicated; this has been observed (15) and a deactivation rate of $4.56 \times 10^9 cm^{-3} mole^{-1} sec^{-1}$ reported. The energy transfer from the first excited state of N_2 to CO_2 may be written symbolically:

$$N_2 (v = 1) + CO_2(00^o0) \longrightarrow N_2 (v = 0) + CO_2(00^o1) - 18\ cm^{-1}. \quad (2.3)$$

Vibrational energy transfer can also occur between higher excited states of N_2 and CO_2 where the energy discrepancies, as implied in equation (2.4) below, are not too large. Patel (11) claims this to be the case up to the v = 6 excited state of N_2. Also, the work of V. N. Kondratyev (16) has indicated that up to v = 4 there is a high probability of transfer due to the relative sizes of ΔE and KT. This transfer reaction can be written:

$$N_2 (v = v') + CO_2(00^o0) \longrightarrow N_2 (v = v' - 1) + CO_2(00^o1) - \Delta E, \quad (2.4)$$

where $\Delta E \gtrsim KT$.

Furthermore, repopulation of the lower levels of N_2 suitable for the transfer reaction with CO_2 can take place as follows:

$$N_2 (v = v') + N_2 (v = v'') \longrightarrow N_2 (v = v' - 1) + N_2 (v = v'' + 1) - \Delta E, \quad (2.5)$$

where $v' > v''$.

The possibility of transfer from N_2 (v = 1) raising CO_2 to levels other than $00^0 1$ is small because of the large energy differences involved. The total result is a very selective excitation of the upper laser levels at rates which have been shown (11) more than capable of yielding the observed high output powers.

Assuming then this highly selective population of the upper laser level, the maintenance of laser action requires depopulation of the lower laser levels ($10^0 0$ and $02^0 0$) at a rate sufficient to satisfy equation (1.9), which defines a state of population inversion. Depopulation of the levels involved in the laser system as indicated in figure one transpires by means of essentially two processes, radiative emission (both spontaneous and stimulated) and collisional energy transfer. To assess the relative importance of these processes it is desirable to know the radiative lifetimes of the relevant states. The lifetime of a given state against spontaneous radiative decay follows directly from a knowledge of the transition probabilities between that state and all other states to which transition by radiative decay is permitted. If the rate per unit time, per transition unit, of transitions between the upper state and a lower state i is p_i, and if the transition rates to these lower states of which there are n are mutually independent, then the total rate per unit time of transitions from the upper state to all lower levels is

$$P = p_1 + p_2 \cdots + p_n. \qquad (2.6)$$

Associated with the process having transition rate p_1 is a lifetime τ_i, where

$$\tau_i = 1/p_i \,. \tag{2.7}$$

It follows directly from (2.6) and (2.7) that the radiative lifetime T^1 of the upper state is determined by the relation.

$$\frac{1}{T^1} = \frac{1}{\tau_1} + \frac{1}{\tau_2} \cdots + \frac{1}{\tau_n} \,. \tag{2.8}$$

The work done on CO_2 vibrational intensities prior to the advent of the CO_2 laser did not sufficiently treat all the transitions of interest, nor was sufficient work done for the determination of parameters which would permit the numerical calculation of transition probabilities. Recently there have been endeavors to obtain the information, but the relatively brief period of increased interest and the great complexities of the problems involved have prevented in full measure the achievement of the desired results. Perhaps the most successful effort thus far is the set of calculations carried out by H. Statz et al (17) employing parameters obtained by comparing certain observed and calculated absorption coefficients. The calculations are far too extensive and complex to be reproduced here, but an indication of the basic procedures should be pertinent.

The Einstein coefficient of spontaneous emission which was introduced in equation (1.1) is specified (18) quantum mechanically by the relation

$$A_{21} = (2J_2+1)^{-1} \ (64\pi^4/3h\lambda^3) S_{21} , \tag{2.9}$$

where J_2 is the angular momentum of the upper level, h is Planck's constant, λ is the wavelength of the emitted photon, and S_{21} is called the line strength or matrix element of the transition. Recall that the subscript 2 refers to the upper level, 1 to the lower. The line strength S_{21} is given by

$$S_{21} = \sum_{M_2 M_1} \left| \left\langle J_2, M_2 \left| \vec{P} \right| J_1, M_1 \right\rangle \right|^2 , \tag{2.10}$$

where J_2 and J_1 refer to the angular moment of the upper and lower states, M_2 and M_1 are their z components respectively, and $\vec{P}$ is the associated dipole operator. The full vibrational-rotational wavefunction implied in the notation of (2.10) for a certain state is given by A. R. Edmonds (19) as

$$\Psi = \left[(2J+1)^{\frac{1}{2}}/2(2\pi)^{\frac{1}{2}}\right] D_{M\ell}^{J}(\alpha, \beta, \gamma) \times \psi^{n1}(\sigma) \psi^{n2,\ell}(\rho) \psi^{n3}(\zeta) . \tag{2.11}$$

The terms $D_{M\ell}^{J}(\alpha, \beta, \gamma)$ are the eigenfunctions of a symmetric top having total angular momentum J, angular momentum ℓ along the figure axis, and z component of angular momentum M. The parameters α, β, γ are the Euler angles, $\psi^{n1}(\sigma)$ and $\psi^{n3}(\zeta)$ are the

conventional Hermitian harmonic oscillator functions, and $\psi^{n2,\ell}(\rho)$ represents a two dimensional harmonic oscillator analog. The variables σ, ζ, and ρ are related to normal coordinates used to describe the normal modes of oscillation of the CO_2 molecule and are defined in reference (17). The problem then is to assume a proper Hamiltonian for the system taking into account the necessary anharmonic contributions, determine explicitly from the Hamiltonian and known energy state values the associated wave function given implicitly in equation (2.11), formulate the proper form of the dipole operator $\vec{P}$ in the suitable coordinate system, and evaluate the matrix elements in equation (2.10). Substituting this result into (2.9) one finds the transition rate A_{21}, which is equivalent to p_i of equation (2.7) where i signifies the transition from state 1 to 2. The lifetime of the upper state follows from equation (2.8) when all the p_i's have been so determined.

The lifetimes of the pertinent states as calculated by Statz et al appear in table one. Contained in the table are values under the heading "Radiation Trapped." When a photon is given off as result of a transition between two energy states it must, assuming it initially is contained in the interior of a laser cavity, travel a finite distance through the plasma before escaping. During this travel it comes in contact with molecules similar to that from which it originated and may be reabsorbed or "trapped." This tends to repopulate the relevant upper level and prolong the life of the state. Radiation trapping is

TABLE 1

CALCULATED LIFETIME (SEC) OF VIBRATIONAL STATES AGAINST SPONTANEOUS EMISSION (17)

	From Experimental Absorption Coefficients		From Theoretical Absorption Coefficients	
Level	Untrapped	Radiation Trapped	Untrapped	Radiation Trapped
$00^{0}1$	2.6×10^{-3}	4.9×10^{-2}	2.4×10^{-3}	5×10^{-2}
$10^{0}0$	0.95		1.1	
$02^{0}0$			1.0	
$01^{1}0$ (J even)	0.93	3.0	1.1	2.8
$01^{1}0$ (J odd)	0.93	0.99	1.1	1.1

especially important in the cases of those states linked directly to the ground level, as the ground level maintains a high population which increases the probability of reabsorption. The values of table one admitting radiation trapping were calculated for a laser cavity similar to the one employed in the experimental work preliminary to the writing of this thesis and to be described in a later section. The method for calculating these values was taken from the text of reference (20).

It is apparent from the values given in table one for the lifetimes of the states that spontaneous emission could not possibly be the mechanism responsible for depopulating the lower laser levels sufficiently to effect a population inversion and maintain laser action. Hence collisional processes, either with the walls or other molecules, must be the depopulating agents. Experiments have indicated that the gain per cubic unit of plasma utilized is relatively unaffected by the tube diameters of the (cylindrical) cavities, and CO_2 lasers have been successfully constructed having tube diameters varying from a few millimeters to a few inches. This seems to be a verification of Patel's early conjecture (21) that optical gain for the CO_2 laser should at most be a slowly decreasing function of tube diameter in contrast to other lasers. Thus one cannot attribute the necessary depopulation effect to wall type collisions. By the process of elimination the mechanism of depopulation of the lower laser states appears to be inter-molecular collision. This is the opinion put forth by H. Statz

et al in reference (17). Experiments employing a He-CO_2 mixture as the active plasma of the CO_2 laser have shown (22) that higher power outputs can be obtained from the addition of He than from the addition of N_2. Because of the relative spacing of energy levels of He and CO_2 it is doubtful that He has a direct effect (in the absence of N_2) in populating the upper laser state. Rather this function is left to other mechanisms (see reference 7), and one may conjecture reasonably that the function of He is to depopulate the lower laser states, possibly by collisional conversion of vibrational energy into translational energy of He.

Epitomizing, there is strong evidence that the mechanism for populating the upper laser level of the CO_2 molecule in the CO_2-N_2 laser is vibrational energy transfer through collisions. The work done thus far on the determination of transition probabilities and the lifetimes of relevant states against spontaneous decay is somewhat incomplete, but that which has been done indicates that spontaneous radiative emission is not sufficient to depopulate lower laser levels and effect the necessary population inversions. A definitive statement cannot be put forth at this time on the means of depopulation, but molecular collisional processes appear appropriate. The fact that the laser operates, and operates continuously, is proof positive that the state of population inversion and the associated mechanisms exist.

The authors of reference (17) have analyzed what they consider a typical situation and concluded, that the ratio of molecules in the upper laser state to those in the lower laser state is about 1.05. This figure will be later substantiated as reasonable.

C. Optical Gain

As mentioned previously, output studies of the conventional CO_2 laser show that oscillation takes place only on a number of P-branch transitions. An analysis of optical gain for the various transitions, based on a development given by Patel (23), explains the observed absence of the R-branch transitions and provides a theoretical basis for employment of a method of selective oscillation.

Consider a parallel beam of electromagnetic radiation advancing in the positive z direction and having a frequency spread from ν to $\nu + d\nu$. It travels through a gaseous medium containing $\delta N_{2\nu}$ atoms per cc, from an upper state population of N_2 per cc, which are capable of emitting radiation in the frequency range of the beam, and $\delta N_{1\nu}$ atoms per cc, from a lower state population of N_1 per cc, which are capable of absorbing radiation in this same range. In propagating through a distance dz it follows from the discussion of Einstein coefficients that the increase in beam energy is given by

$$d\left[I_\nu \delta\nu\right] = \delta N_{2\nu} \frac{dz}{c} h\nu \, B_{21} I_\nu - \delta N_{1\nu} dz \, h\nu \, B_{12} \frac{I_\nu}{c} . \qquad (2.12)$$

Spontaneous emission has been left out here as it is given off in a random direction and contributes a neglible energy addition to the beam. Rewriting equation (2.12), one may obtain

$$\frac{1}{I_\nu}\frac{dI_\nu \delta\nu}{dz} = \frac{h\nu}{c}\left(B_{21}\ \delta N_{2\nu} - B_{12}\ \delta N_{1\nu}\right). \tag{2.13}$$

Comparing equation (2.13) with equation (1.5) it is seen that the left-hand side of the former can be equated to $-k_\nu \delta\nu$. It is now advantageous to define the gain or emission coefficient as

$$\alpha_\nu = -k_\nu , \tag{2.14}$$

and to rewrite for clarity equation (1.6) in terms of this new coefficient:

$$I_\nu = I_o\, e^{\alpha_\nu z}. \tag{2.15}$$

Hence equation (2.13) yields

$$\alpha_\nu d\nu = \frac{h\nu}{c}\left(B_{21}\ \delta N_{2\nu} - B_{12}\ \delta N_{1\nu}\right). \tag{2.16}$$

Integrating both sides of this expression over the entire emission line, one finds

$$\int \alpha_\nu d\nu = \frac{h\,\nu_o}{c}\left(B_{21} N_2 - B_{12} N_1\right), \tag{2.17}$$

where the slight variation in ν has been neglected on the right-hand side and denoted with a zero subscript referring to the value at the center of the line. Employing equations (1.3) and (1.4) to rewrite (2.17) in terms of Einstein's coefficient of spontaneous emission we have finally

$$\int \alpha_\nu d\nu = \frac{\lambda_o^2 g_2}{8\pi} A_{21}\left[\frac{N_2}{g_2} - \frac{N_1}{g_1}\right]. \tag{2.18}$$

Note that equation (2.17) is an equivalent form of the Füchtbauer-Ladenburg formula, equation (1.7), which was previously assumed without derivation.

An emission line which is the result of transitions between a certain pair of energy states has a finite linewidth due to various broadening effects. Since in the case of a laser the line is the result of induced emission, natural broadening, which is directly related to the lifetime of the upper state against spontaneous emission, has but a minor effect. Furthermore, gas pressure in the CO_2 laser is typically a few torr, whereby collision boradening also plays only a secondary part. It can be assumed that Doppler broadening is primarily responsible for the linewidth. According to Mitchell and Zemansky (24) it is a "well-known result" that for a primarily Doppler broadened line the gain coefficient of a gas is given by

$$\alpha_\nu = \alpha_o \exp- \left[\frac{2(\nu - \nu_o)}{\Delta\nu_D} \sqrt{\ln 2} \right]^2, \qquad (2.19)$$

Actually this equation was originally given in terms of the absorption coefficient k_ν, but it has been modified by application of relation (2.14). The quantity $\Delta\nu_D$ is the Doppler width at half power and is given in terms of the molecular temperature T_{mol} and the molecular mass M by the formula

$$\Delta\nu_D = \frac{2\sqrt{2K\ln 2}}{c} \nu_o \sqrt{\frac{T_{mol}}{M}}, \qquad (2.20)$$

where K is Boltzmann's constant and ν_o is frequency at the center of the line. In equation (2.19) the quantity α_o is the maximum gain coefficient and corresponds to the frequency ν_o. Now, integrating equation (2.19) over all frequencies yields

$$\int \alpha_\nu d\nu = \frac{1}{2} \sqrt{\frac{\pi}{\ln 2}}\ \alpha_o\ \Delta\nu_D \,. \tag{2.21}$$

The left-hand sides of this equation and equation (2.18) are identical. Equating the right-hand sides and solving for the maximum gain coefficient, where the subscripts "21" replace the subscript "0" to indicate the transitions take place between the upper and lower energy state respectively, one obtains:

$$\alpha_{21} = \sqrt{\frac{\ln 2}{\pi}}\ \frac{g_2 A_{21}}{4\pi} \left(\frac{N_2}{g_2} - \frac{N_1}{g_1}\right) \frac{\lambda_{21}^{\,2}}{\Delta\nu_D} \,. \tag{2.22}$$

The time required for thermalization of the rotational levels in the upper laser state has been given to be of the order of 10^{-6} to 10^{-7} seconds (14, 25). The lifetime against spontaneous decay has previously been given as greater than 10^{-3} seconds, and Statz et al (17) have performed a calculation from which one might infer that a typical lifetime for the upper state under laser activity would be of the order of 10^{-5} seconds. Comparing these figures it follows that even in a laser situation the upper state maintains thermal equilibrium amongst the rotational levels, that is a Boltzmann distribution. In such a case

Herzberg (10) shows that the population density of the Jth rotational level is given by

$$N_J = (N/Qr)\, g_J \exp\left[-F(J)\, hc/K\, T_{rot}\right], \tag{2.23}$$

where $N = \sum_J N_J$, Q_r is the rotational partition function, and F(J) is the energy of the Jth rotational level from the energy the state would have neglecting rotational contributions. Specifically

$$F_J = BJ(J+1) - DJ^2(J+1)^2 . \tag{2.24}$$

Now for linear polyatomic molecules the rotational partition function is given as

$$Q_r = \sum_J (2J+1) \exp\left[-F(J)\, hc/K\, T_{rot}\right] . \tag{2.25}$$

In the present case where B is small and T comparatively large, Q_r may be approximated as

$$Q_r \approx K\, T_{rot}/hcB, \tag{2.26}$$

whereby (2.23) becomes

$$N_J = N\,(hcB/K\, T_{rot})\, g_J \exp\left[-F(J)\, hc/K\, T_{rot}\right] . \tag{2.27}$$

It is here convenient to rewrite equation (2.9), specifying the method of calculating the Einstein coefficient for spontaneous emission, in the following form:

$$A_{2_J\,1_{J\pm1}} = (64\,\pi^4\,\nu^3_{2_J\,1_{J\pm1}}/3h\,g_J)/R_{21}S_J. \tag{2.28}$$

The index J here refers to the upper state J value; the lower state value is then $J \pm 1$ according to selection rules (2.2). Also the statistical weight of the upper level $(2J+1)$ has here been written implicitly

as g_J. The linestrength or matrix element for the transition, which was denoted S_{21} in equation (2.10), is here divided after Herzberg (10) into a J-dependent part S_J and a J-independent part R_{21}. Substituting equation (2.20), (2.27), and (2.28) into equation (2.22) one obtains

$$\alpha_{2_J 1_{J\pm1}} = \frac{8\pi^3 c^4 R_{21}}{3KT_{rot}(2\pi KT_{mol}/M)^{1/2}} S_J \left[N_2 B_2 e^{-F_2(J)hc/KT_{rot}} - N_1 B_1 e^{-F_1(J\pm1)hc/KT_{rot}}\right]. \tag{2.29}$$

Now, following Patel, the somewhat liberal assumption is made that

$$T_{mol} \approx T_{rot} \equiv T. \tag{2.30}$$

Then for P-branch transitions where $S_J = J+1$ the optical gain, i.e. equation (2.29) becomes

$$\alpha_{2_J 1_{J-1}} = \frac{8\pi^3 c^4 R_{21}(J+1)}{3KT(2\pi KT/M)^{1/2}} \left[N_2 B_2 e^{-F_2(J)hc/KT} - N_1 B_1 e^{-F_1(J-1)hc/KT}\right], \tag{2.31}$$

and for R-branch transitions where $S_J = J$, equation (2.29) becomes

$$\alpha_{2_J 1_{J-1}} = \frac{8\pi^3 c^4 R_{21} J}{3KT(2\pi KT/M)^{1/2}} \left[N_2 B_2 e^{-F_2(J)hc/KT} - N_1 B_1 e^{-F_1(J-1)hc/KT}\right]. \tag{2.32}$$

These equations for optical gain are quite general and can be applied to any linear polyatomic molecule system. If the necessary parameters were known, one could calculate by means of equations (2.31) and

(2.32) the optical gain as a function of the upper state J value for the P and R branch transitions respectively. All the necessary parameters are known with the exceptions of the vibrational state populations N_1 and N_2, and the characteristic temperature T. Performing calculations based on this development, Patel (7) concluded that a reasonable T value is 400° absolute. Using this figure and assuming various appropriate inversion ratios, i.e. N_2/N_1, Patel and his coworkers (23) programmed a computer to plot equations (2.31) and (2.32) expressed in arbitrary units as functions of upper state J values for the $00^{\circ}1$-$10^{\circ}0$ band. The resulting graph is reproduced in figure two.

Referring to the figure, two important conclusions can be drawn. First, as expected, the gain on any certain transition increases rapidly with increasing population inversion. Second, for any given population inversion ratio the P-branch transitions show substantially higher gain than the R-branch transitions. Furthermore, this holds true not only in the comparison of transitions starting in the same upper rotational level, but for particular P and R-branch transitions in general. These concluded results both explain the absence of the R-branch lines in the output of a conventional CO_2 laser, and predict the ability of a selective process of oscillation to produce many of the unseen lines. Analysis of a hypothetical situation is perhaps the best way to make this clear. Since the wavelengths characteristic of transitions belonging to the same rotation-vibration band are closely

FIG. 2: Normalized Optical Gain

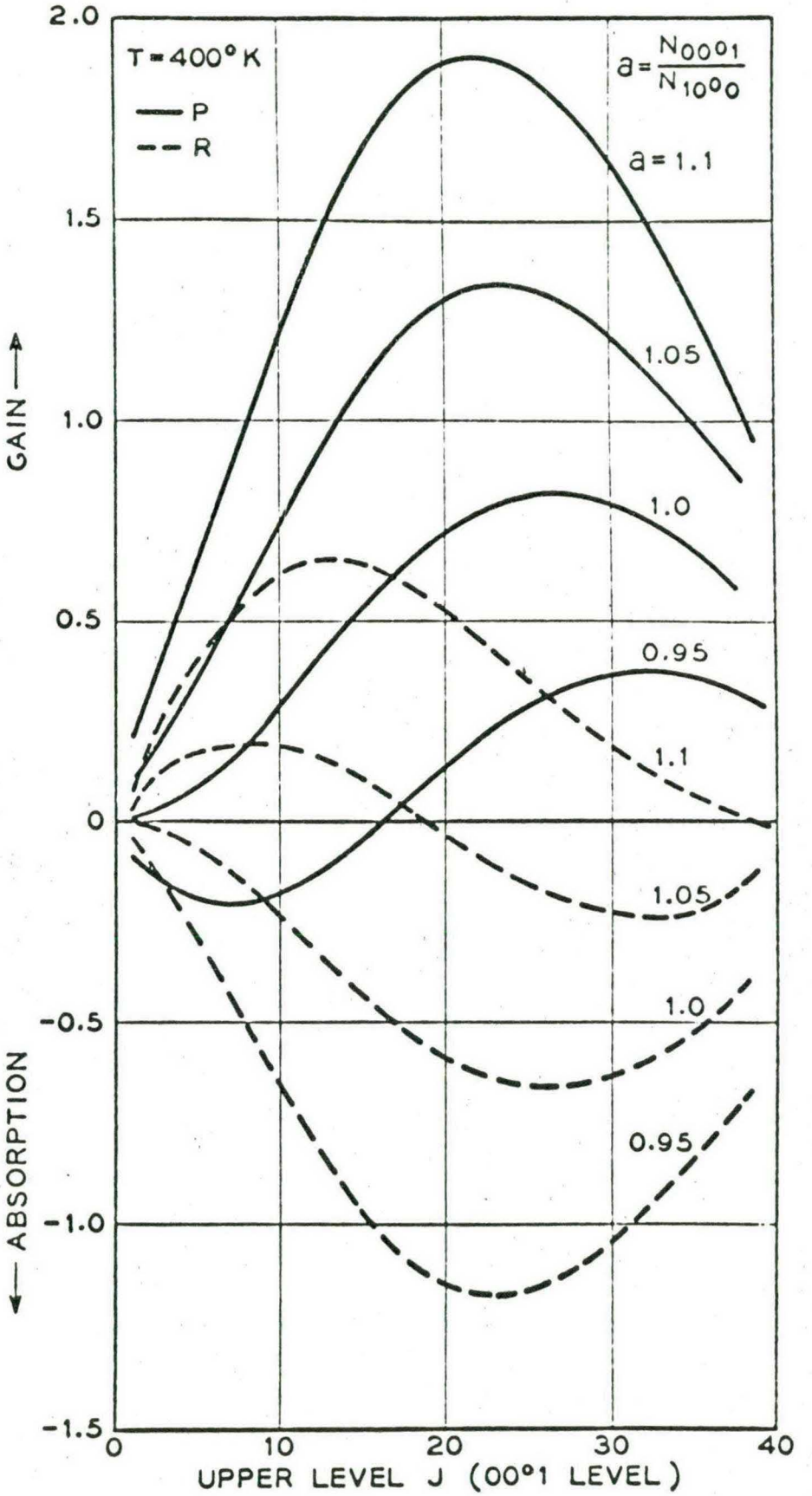

spaced, it can be assumed in a first approximation that all the lines resulting from these transitions suffer the same percentage dissipative losses per transit of the laser tube. Let us assume a laser which has no method of selective oscillation, but can be Q-switched. The quality factor "Q" of the resonant cavity can be defined by the equation

$$Q = \frac{2\pi\nu(Mh\nu)}{P^*}, \tag{2.33}$$

where M is the number of photons of energy $h\nu$ stored within the cavity, and P^* is the rate of power dissipation. Suppose that the losses inherent in the tube and wavelength combination are such that a gain of 1.0 or greater on the scale of figure two is required to maintain laser action on any given line when the Q of the tube is in the high position. The laser is continuously excited and initially switched to low Q, such that laser action is inhibited. In the absence of stimulated emission the population inversion ratio quickly reaches its maximum value for the tube geometry and conditions, say 1.5. Switching to high Q, induced transitions immediately lower the inversion ratio to a steady state value of, let us assume, 1.05. Examining the curves in figure two plotted for the 1.05 inversion ratio it is apparent that only P-branch transitions having an upper state J value in the range 14 to 34 are able to sustain oscillation; the R-branch transitions are totally absent. If the steady state population inversion ratio were reduced by

the laser action to a value of 1.03, only one or two P-branch transitions in the neighborhood of J = 24 might be seen. Now suppose a process of selective oscillation is incorporated into the laser, a process wherein the Q of the laser cavity may be switched to the high position for a single given line. Since the inversion ratio necessary for oscillation is inversely proportional for any certain line to the Q of the cavity (26), only the single line may oscillate. Assuming that for the maximum population inversion ratio of 1.5 a particular line has sufficient gain to initiate oscillation, it follows that since only this line oscillates the steady state population inversion ratio cannot be reduced to a level where the particular line fails to appear. Hence, under selective oscillation many lines will appear from both P and R branches which are not seen during non-selective operation.

D. The Resonant Cavity

The resonant cavity of a gas laser functions as a feedback circuit to the amplifying medium. Usually it takes the form of two spherical mirrors mounted upon a common optic axis and focused to reflect the desired radiation back through the amplifying medium where it originated. The amplifying medium is normally contained in a glass or quartz tube of suitable dimensions, and the mirrors may be mounted either external or internal to this tube. In the case of externally mounted mirrors the tube is best terminated by flat windows,

optically capable of passing the desired radiation, and mounted at Brewster's angle to insure maximum passage in one field polarization. For most gas lasers, notably those employing noble gases, over a suitable region the gain is inversely proportional to tube diameter. This occurs as wall-molecule collisions are important in depopulating lower laser energy levels. In the case of CO_2, however, experiment has shown gain to be roughly independent of tube diameter as long as it is sufficiently large to permit transfer of the oscillating beam.

In order to obtain the high Q values (cf. equation 2.33) necessary to effect oscillation, the mirror design and configuration must be such that paraxial radiation is constrained within the optical cavity. Kogelnik and Li (27) have shown on the basis of geometrical optics that this stable or low-loss situation exists when the parameters of the system satisfy the relation

$$0 < (1 - \frac{d}{R_1})\ (1 - \frac{d}{R_2}) < 1\ , \qquad (2.34)$$

with d being the mirror separation and R the mirror radius of curvature. The R value is taken as positive when the mirror is concave, negative when convex. Of the various possible stable systems it is pertinent here to mention specifically that system wherein both mirrors have a positive radius greater than the mirror separation. Another is that system formed by a concave mirror with radius greater than the mirror separation and opposed by a plane mirror, one having an infinite R value.

The periodicity and boundary conditions inherent in the resonant system permit maintenance of only certain modes of oscillation dependent upon the cavity parameters and the wavelength of oscillating radiation. For the symmetric situation, both mirrors having the same radius of curvature, Boyd and Kogelnik (28) have shown the following equation must be satisfied:

$$\frac{2d}{\lambda} = q + \frac{1}{\pi} (2p + m + 1) \cos^{-1} \left(1 - \frac{d}{b}\right) , \qquad (2.35)$$

where p and m are the transverse mode numbers, q is the longitudinal mode number. In general, more than one mode of oscillation will be present at a given time within a laser cavity. The stability condition (equation 2.34), derived on the basis of geometrical optics, neglects the effects of diffraction losses. It has been shown (29, 30) that minimum diffraction loss occurs for the lower transverse modes of oscillation; lower diffraction losses imply higher Ω value and dominant operation. However, lower transverse modes produce beams confined to smaller cross sections of the laser tube, and hence possibly smaller absolute gain. In fact, Rigrod (31) found experimentally that higher order transverse modes operate preferentially over lower order modes when cavity dimensions are permitting. If the beam widths of the various modes are comparable to the tube diameter or the face diameters of the mirrors, the lowest order transverse modes, which suffer the least interference, can be expected to oscillate. The possible

lowest order transverse or uniphase modes which may oscillate are found from equation (2.35) when p and m are set to zero. The resulting relation may then be written in a more convenient approximate form:

$$d = \frac{q\lambda}{2} . \tag{2.36}$$

This equation shows the mirror separation must be approximately equal to an integral number of half-wavelengths.

The uniphase mode is known to have a gaussian intensity distribution in any cross section. In this case, that is -- for a gaussian distribution, it is advantageous to describe the width of the beam in terms of the "spot size," the cross-sectional radius w at which the electric field intensity falls to 1/e of its maximum value. The spot size is a function of distance s along the optical axis of the cavity from the beam waist, whereat the beam wavefront is planar and the spot size w_o is a minimum. Reference (27) shows this dependency to be

$$w^2(s) = w_o^2 \left[1+\left(\frac{\lambda s}{\pi w_o^2}\right)\right]^2 . \tag{2.37}$$

For the symmetric mirror configuration the beam waist is located at the geometrical center of the cavity; the parameter w_o can be calculated from the relation

$$w_o^2 = \frac{\lambda}{2\pi}\left[d\,(2R - d)\right]^{1/2} . \tag{2.38}$$

The configuration of one concave and one flat mirror in analogous, with the exclusion of certain modes of oscillation, to a symmetric

configuration having two concave mirrors identical to the original, and a cavity length twice as long. Multiplying each d in equation (2.38) by two, the formula for calculating w_o in the second situation is found:

$$w_o^2 = \frac{\lambda}{\pi} \left[d(R - d)\right]^{1/2} . \tag{2.39}$$

By analogy the beam waist is in this case located at the plane mirror.

The number of longitudinal modes which oscillate in a given cavity is dependent upon the Doppler width of the line in question, the spacing of successive longitudinal modes, and the gain threshold for oscillation. The Doppler width can be calculated from equation (2.20) by inserting the proper parameters. The mode spacing, which is characteristic of the cavity length d, can be calculated from the following equation which is derived from equation (2.36) in a straight forward manner.

$$\Delta\nu_R = \frac{c}{2d} . \tag{2.40}$$

In order to obtain oscillation on a given transition equation (2.36) must be satisfied. Because of the small wavelengths typical of optical spectra, it is very difficult to "tune" the length of a cavity to satisfy (2.36) for a given λ and a given q. Furthermore, thermal transients within the cavity apparatus cause the length to undergo constant alteration of sufficient magnitude to frustrate satisfaction of (2.36) for specified parameters. If, however, the Doppler width is large compared to the separation of successive modes, and the gain threshold is

sufficiently below the gain peculiar to most elements of the Doppler broadened line (recall that gain is highest at the line center), a number of these modes will be able to oscillate at any given time regardless of cavity length variation. If the mode spacing is comparable to the Doppler width or smaller, a minimum number of modes only, say one or two, will be capable of oscillating. Perhaps for a given situation no mode of oscillation will occur during transient periods. This latter situation gives rise to high instability of intensity on any given line in the output spectrum. This instability is a problem, as will be shown later, with the typical CO_2 laser. One method of minimizing it is to increase the length of the cavity, thereby decreasing the mode spacing and guaranteeing the oscillation of one or more modes for any cavity length perturbation.

E. The Mechanism of Selective Oscillation

The function of the selective oscillation mechanism is to discriminate on the basis of wavelength against unwanted transitions, and nullify laser action on them. The obvious method of achieving this function is to incorporate in the cavity a dispersive element capable of directing the various wavefronts, each one being characteristic of a certain transition, along separate paths. The element must be tunable, so that high loss can be selectively introduced into oscillations over

all paths except that of one desired wavefront. Two such elements are the prism and the diffraction grating. The components of a vibration-rotation band branch are relatively closely spaced in energy and hence in wavelength, requiring high resolving power to effect separation through dispersion. On this basis the diffraction grating is the better suited element.

When a parallel, monochromatic light beam is incident upon a plane diffraction grating, the reflected beams of various orders consist also of parallel rays. This is a case of Fraunhofer diffraction. Using a suitable grating, properly orientated, to terminate one end of the CO_2 laser cavity, the first order diffraction maxima of the various band components will be given off in a plane perpendicular to the face of the grating, and at divergent angles to one another. By rotating the grating about an axis passing perpendicularly through the axis of the cavity and the plane of diffraction, a particular band component may be made to have its incident and first order diffracted beam coincide. Other things assumed, the energy of this one beam is sufficiently confined within the cavity to maintain laser action, while the beams of the remaining elements spew their energy out of the cavity into the surrounding space. For the particular beam the grating acts as a plane mirror oriented perpendicularly to the cavity axis.

The "other things assumed" mentioned above are specifically that the resulting cavity be stable, the resolving power and angular

dispersion of the grating be sufficient to separate out the unwanted components, and the percentage of incident beam intensity reflected in the first order diffraction maximum be high enough to establish laser oscillation. A necessary criterion for a stable cavity was given above as the satisfaction of equation (2.34). Since the grating acts for the selected component effectively as a plane mirror, the criterion requires the other end of the cavity be terminated by a concave spherical mirror having a radius of curvature greater than the cavity length d. The beam waist is then located at the grating, whereby the incident and emerging wavefronts are planar as was assumed previously.

In almost any textbook on introductory physical optics such as that by Jenkins and White (32) a relation is derived theoretically giving the maximum intensity distribution of the Fraunhofer diffraction pattern of an ideal grating, which may be given as follows:

$$I = a^2 \frac{\sin^2 N\eta}{\sin^2 \eta}, \tag{2.41}$$

where N is the number of slits upon the grating which take part in the forming of the pattern and

$$\eta = \frac{\pi b}{\lambda} (\sin\Theta + \sin i). \tag{2.42}$$

Here a^2 is the intensity pattern from any one single slit, b is the slit spacing, i is the angle of incidence measured to the grating normal, and Θ is the angle between the grating normal and a vector directed towards the diffracted wavefront whereat the intensity is to be

determined. In the ideal case the factor a^2 is the intensity distribution of a single slit diffraction pattern. It can easily be shown that the principal intensity maxima occur at angular positions which satisfy the relation

$$b\,(\sin\Theta + \sin i) = m\lambda\,. \tag{2.43}$$

For a fixed angle of incidence, the angular dispersion is obtained to a high approximation by differentiating equation (2.43) and substituting small increments for the differentials:

$$\frac{\Delta\Theta}{\Delta\lambda} = \frac{m}{b\cos\Theta}\,. \tag{2.44}$$

Referring now to the selective cavity, if a beam is spaced in wavelength by $\Delta\lambda$ from that beam for which the cavity is focused, then the lateral displacement at the concave mirror of this beam from the position of focus is

$$\Delta x = d\,\Delta\Theta = \frac{d\,\Delta\lambda}{b\cos\Theta}\,, \tag{2.45}$$

where we are speaking now of the first order maximum only. Having a specific grating and assuming a criterion for Δx, this last equation can be used to determine the necessary cavity length d for effective oscillation.

Referring again to an introductory text, the theoretical resolving power of a grating, based on the Rayleigh criterion that for two just

resolved lines the maximum intensity point of one fall at the first minimum of the other, is given as

$$\text{Resolving Power} = mN = \lambda/\Delta\lambda. \tag{2.46}$$

It is well to note here that a laser equipped with a selective oscillation mechanism would tend to amplify a line when the cavity is focused well, but perhaps not at all when the cavity is slightly misfocused. If the cavity were focused to oscillate at the frequency of the cross over point of two just resolved lines, then because of the intensity loss per cycle of oscillation the laser output would show at best severly reduced amplification. Effectively, the resolving power of the grating would be enhanced, whereby it follows that the Rayleigh criterion may be overly demanding.

In order to satisfy the requirement that a high percentage of incident energy intensity is concentrated into a given diffraction maximum, an echelette type grating is called for. These gratings have their slit faces inclined at an angle to the grating plane such that geometrical reflection favors the desired direction, this direction being for a given wavelength that of the desired order. Echelette gratings operating in the infrared have been constructed capable of concentrating more than 90% of the incident radiation into the desired order.

In the case of a real grating, equation (2.41) is still valid; however the factor a^2 cannot be given correctly by the single slit diffraction pattern intensity distribution. In general a^2 is a complex

distribution peculiar to the method of drawing the grating, or perhaps even the individual grating itself. The best that may be said in lieu of more exact information given by the manufacturer, is that the intensity is maximum in the direction normal to the face of the slit, and decreases gradually over small increments in angle to either side of this normal. Hence, if the echelette grating were used with wavelength slightly different from that for which the grating is "blazed" (the blaze angle being the angle between the grating normal and the slit face normal), the percentage intensity concentrated into the appropriate maximum would be high, but somewhat less than that given by the manufacturer for use with the proper wavelength.

In conclusion the cavity length, mirror radius, and grating can be selected on the basis of the above discussion to match resolving power and angular dispersion to cavity dimensions for achievement of selective oscillation. With an echelette grating of the proper blaze, used on the high gain CO_2 laser, there should be small difficulty in achieving oscillation. In an extremely efficient system a problem might be the protection of the grating surface against destructive heating effects. On the other hand, in less efficient atomic lasers diffraction loss from the grating would perhaps preclude oscillation. In the final analysis, the only vindication of the ability of a selective system to achieve laser oscillation and perform as intended is that of experimental success.

III. EXPERIMENT

A. Apparatus

The principal element physically of the CO_2 laser is of course the discharge tube. The particular tube employed in these investigations was constructed from pyrex glass tubing have a 15 mm outside diameter, and an inside diameter of about 12.5 mm. The length was approximately 165 cm, with one end sawed perpendicularly to the axis, the other at Brewster's angle. To this basic structure was blown a centrally located large-diameter exhaust port and stopcock, and two somewhat smaller diameter inlet ports and associated stopcocks. These last were spaced symmetrically, each 75 cm from the exhaust port. The stopcocks were in turn blown to the socket halves of ball and socket joints, for easy connection to appropriate filling and exhausting apparatus. Also blown onto the tube, in the same plane and on the side opposite the gas ports, were two cold cathode neon-sign type electrodes. These also were spaced symmetrically to the tube center, and at a separation of 135 cm. The tube was supported upon and insulated from a two meter optical bench by means of machined plexiglass holders. In its relaxed state the tube was slightly bowed, whereby it was advantageous to deform the tube, by action of the clamping mechanisms inherent in the holders, so as to obtain the maximum

diameter optical path through the tube bore. Holding the tube in position under stress had the further advantageous effect of eliminating the susceptibility to misalignment, relative to other laser components, as the result of light accidental jarring.

Onto the end of the tube sawed angularly was cemented with a compound called "Torr Seal" a stainless steel receptacle designed to hold a sodium chloride window, 6 mm thick and 5 cm in diameter. When put in place the window rested upon an O-ring, which was located in an appropriate seat. Evacuating the tube caused the O-ring to compress, by virtue of the atmospheric pressure exerted on the window exterior, forming a vacuum tight seal. The receptacle had been drilled so that when in place the optical path of the tube continued uninhibited through the receptacle and window combination. The receptacle held the window at the same angle at which the tube was cut, Brewster's angle (33). It is in general the angle of incidence for radiation at which transmission is maximum (100%) in the polarization having a component normal to the window. This compares to transmission at normal incidence where a reflection loss of about 4% is suffered in each polarization. Brewster's angle is a function of the indices of refraction for the media bordering the interface and also of the wavelength of radiation. Calculated for 10.6 microns crossing a vacuum to sodium chloride interface, Brewster's angle takes the value 56.3°. Actually deviations of a couple degrees or less to either side of this value result in an

insignificant reduction in transmitted intensity, especially insignificant for the case of the high gain CO_2 laser.

The tube end cut perpendicularly to the axis was inserted into a machined brass mirror enclosure. Part of the enclosure assembly consisted of a mechanism which clamped an O-ring seal about the circumference of the tube, forming a vacuum tight seal with the assembly. The mirror within the enclosure was held by means of the seal internal to the discharge cavity, with a 12 mm diameter face exposed to the optical path. The enclosure itself was threaded into a commercial mirror holder, effectively mounting it on two sets of precision gimbals. These provided limited rotation of the mirror about two perpendicular axes, one vertical and one horizontal, intersecting at and lying in a plane tangent to the central point of the face. The rotational positions could be set or changed very accurately through the adjustment of two micrometer caliper type gauges magnetically coupled to the gimbals. When joined to the tube the O-ring seal easily permitted sufficient rotation of the enclosure to effect mirror alignment, while still maintaining vacuum. The commercial mirror holders were bolted securely to an insulating base formed by layers of glass and plexiglass cemented together, which was in turn rigidly attached to the optical bench by an appropriate support. It was found in earlier experiments with a preliminary tube that less sturdy mirror holders exhibited a collapsing effect when the tube was placed under vacuum, and suffered severe

position deviations as the result of heating effects within the tube. The O-ring seals were capable of sliding along the tube to absorb expansion, but exerted pressures through the O-ring were still sufficient to change alignment and mode tuning. The rigid support by the means just described alleviated these problems to a degree sufficient to facilitate alignment and its maintenance, although mode tuning drifts were still in evidence.

Four different gold-coated, first-surface mirrors plus a diffraction grating were used in various arrangements to terminate the cavity. All of these units were of circular circumference 1-1/2" in diameter and of various thicknesses. All were capable of being inserted either into the brass enclosure described above or into the commercial holders directly. Two concave mirrors having radii of curvature of $3.04 \pm .02$ m and $11.48 \pm .15$ m respectively were used in the internal position. Both of these mirrors had centrally drilled 2 mm diameter holes for coupling radiation out of the cavity. The brass enclosures were fitted with interchangeable stainless steel butt plates, one of which incorporated a KRS-5 window for transmission of the radiation to the exterior after exiting through the drilled holes of the mirrors. This window was also vacuum sealed by means of an O-ring and was orientated perpendicularly to the tube axis. A third concave mirror having radius of curvature equal also to $3.04 \pm .02$ m, but not centrally drilled, was inserted into a

brass enclosure and holder-support combination as described above and used in the external position. The O-ring seal and transmission window adapters were absent from the external assembly. The fourth mirror, a flat, was inserted directly into one of the commercial mirror holders and used primarily to extend the cavity, as described below, rather than to terminate it. The radii of the concave mirrors were measured to the limits of accuracy specified by means of an optical tester employing Ronchi's method (34).

The diffraction grating had a ruled area 3 cm square centered on the 1-1/2" diameter face. The ruling contained 75 grooves per mm with a blaze angle of 26° 45', giving maximum intensity in the first order at 12 microns. The grating efficiency minimum was measured to be 76% in the sixth order at 2 microns. In the sixth order at 1.95 microns the efficiency minimum was given as 69%. A rough estimate of efficiency for the first order of 10.6 microns might then be 50%. The resolving power of the grating was given to be 78% of the theoretical. The grating was inserted into a commercial mirror holder as described above, and positioned relative to the holder so that rotational adjustments would revolve the grating about a central point in its face. The micrometer gauge which controlled rotation about a vertical axis of the gimbals was fitted with a direct drive gear to enable coupling this adjustment to a multiratio gearmotor capable of exactly reproducible speeds. Driving the adjustment through the gear coupling

enabled rotation of the grating at approximately constant angular velocity about a vertical axis through its face.

Because it was desirable to vary the cavity length over a sizable distance, a ten foot aluminum I-beam was employed as an optical bench and set at a distance of about two feet from the track holding the tube. It was set perpendicular to the tube and directed at the end of the track just beyond the Brewster window. Placing the flat mirror at this point of direction on the track and orientating it at a 45^{o} angle to the tube axis, the optic axis of the laser could be effectively continued along and above the I-beam. Placing either the grating or one of the mirrors on a support designed to fit the I-beam, the cavity length could be extended to a maximum of almost six meters. Figure three is a photograph of the laser in its entirety showing the various mechanical elements and their positioning. Figure four is a photograph of the grating and its holder positioned on the I-beam, with the driving motor behind and coupled to it.

Gases were supplied to the tube from a tank each of high grade nitrogen and carbon dioxide. The tanks were connected by means of rubber tubing directly through pressure regulators to separate flow gauges, which served merely as regulating valves. No effort was made to measure rates of flow with these gauges. Outlet tubes from these gauges were joined to a common tube by means of a T-joint and connected by means of a second T-joint to both a vacuum pressure

Figure 3

The CO_2 gas laser set up for selective oscillation. On the extreme left sits the internal mirror and its holder incorporating the mechanism for coupling radiation out of the tube. On the extreme right is seen the I-beam used as an optical bench for extending cavity length, with the grating, its holder, and drive mechanism sitting upon it.

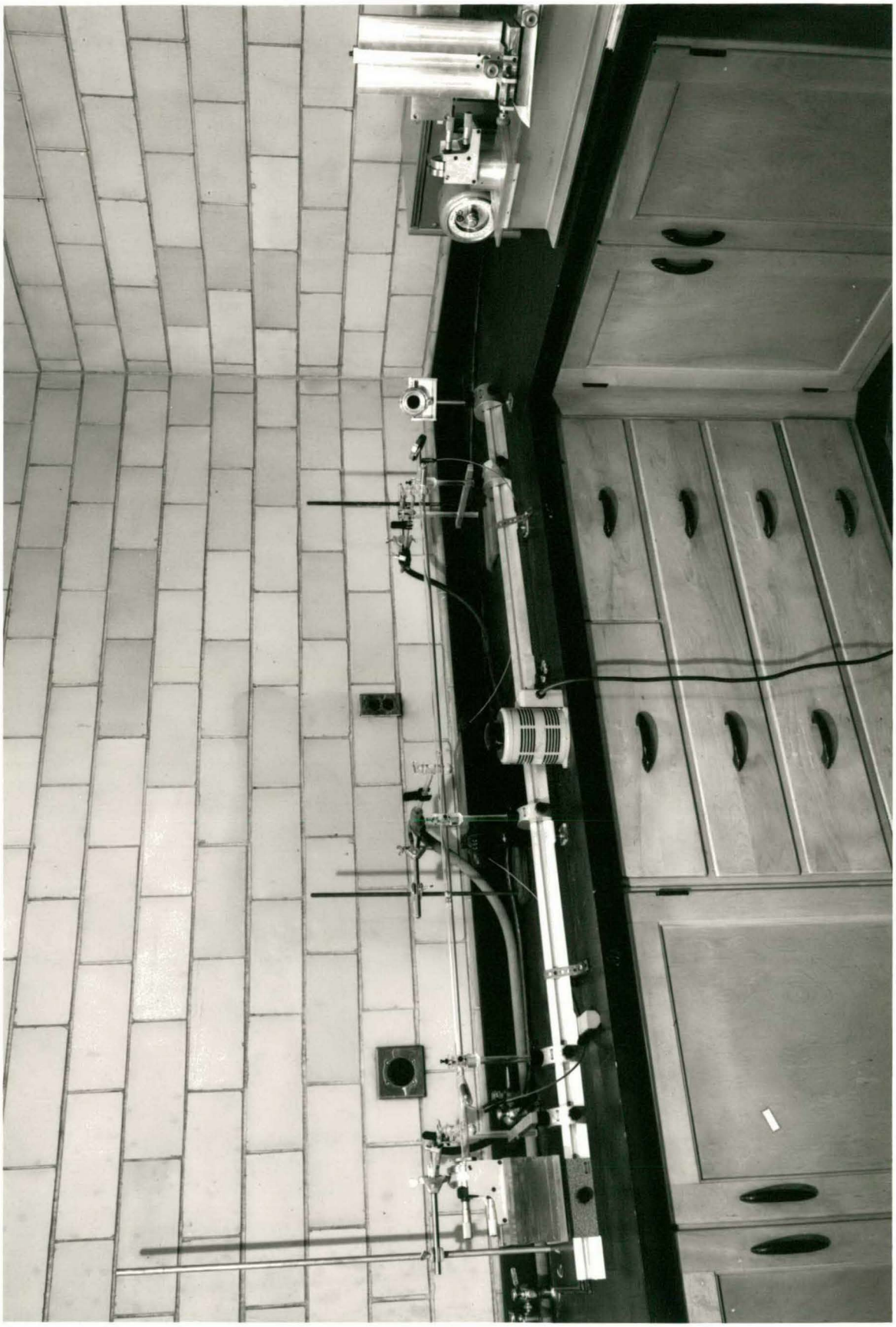

Figure 4

A close view of the grating, its holder, and the multi-ratio gearmotor used to drive the grating when "scanning" the laser lines. The gearmotor is held by an adjustable support which facilitated coupling of the motor to the grating with the absence of unwanted torques.

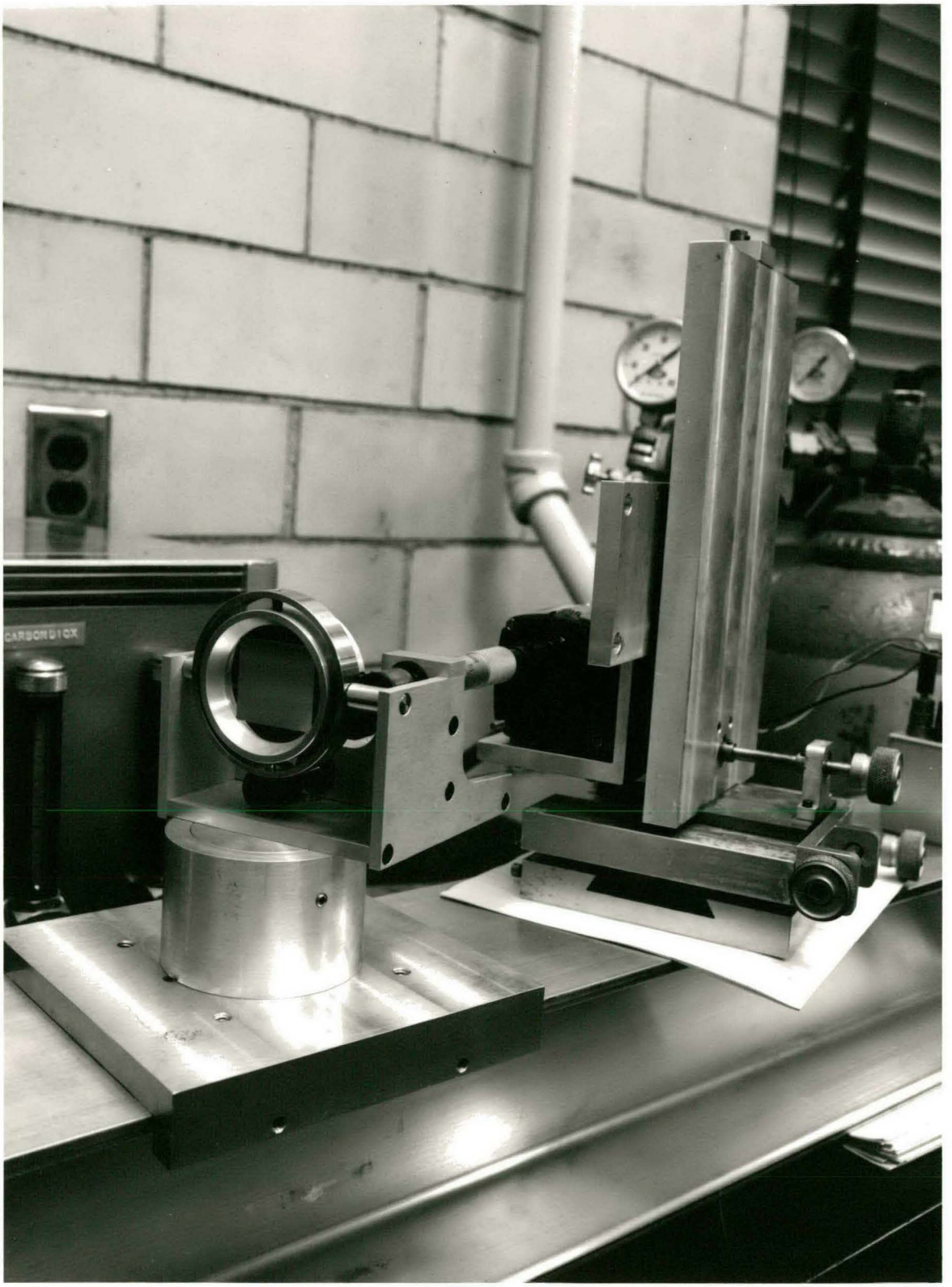
CARBON DIOX

gauge and to a rubber tube leading to the laser. The vacuum gauge was a diaphragm type capable of reading pressures from zero to six hundred torr. It is estimated that in the lower range the gauge was capable of reading pressures accurately to within one-half torr or better, which was sufficient for the intended purposes. The tube leading to the laser connected to a third T-joint and thereby to the two inlet ports. The tubular distances from the gas tanks to the inlet ports were made equal to provide similar inlet pressures at the laser. The exhaust port was connected through heavy rubber tubing to a high-volume, oil-reservoir floor pump, easily capable of maintaining a zero reading upon the pressure gauge when the inlet ports were closed. During laser operation the inlet and exhaust ports were left open permitting a continuous flow of gases at pressures controlled by inlet valve settings.

The laser tube electrodes were connected to an ac luminous tube transformer. The transformer was designed for an input of 120 volts or less, had a maximum output of 15,000 volts, and was rated at 60 milliamps. The power cord of this transformer was connected to a variable transformer "Powerstat" supplying an output voltage of 0-140 volts and capable of 7-1/2 amps. This variable transformer was connected to a common 60 cycle, 120 volt wall outlet.

For the detection and identification of the laser output two methods were employed. In the first, the radiation passing out of the

cavity by means of the hole through the center of the internal mirror was reflected with first surface mirrors into a Perkin-Elmer model 16U grating spectrograph. This instrument indicates mechanically the approximate position of the line being recorded. In the region of ten microns the accuracy was within a few wavenumbers. A second method consisted of permitting the output radiation to impinge directly upon a thermocouple, which was connected through an amplifier to a Brown recording potentiometer. Actually the amplifier and potentiometer were part of a Perkin-Elmer model 12B infrared spectrograph. The exact identification of CO_2 band components could be facilitated by inserting into the path of the output radiation an absorption cell containing ammonia gas, which has a number of strong absorption lines in the proper region. The particular cell used was about 30 cm in length, had an internal diameter of 5 cm, and incorporated sodium chloride transmission windows. The cell could be used in conjunction with both methods of detection. In situations where the output intensity of the laser was too great to send into the detecting instruments, one or two layers of polyethylene sheeting, each 2.7 mm thick, were used for attenuation. Rough tests showed that each layer attenuated the incident radiation to about ten percent of the incident value.

B. Initiating Laser Action

Perhaps the most critical part of setting up a laser for operation is aligning the mirrors. Normally the shorter the cavity length, the less critical the adjustments become. Hence in this experiment the particular cavity initially aligned consisted of two concave mirrors spaced at the minimum separation distance, about 175 cm. The mirror placed in the internal position was that with the longest radius of curvature, 11.5 m; the opposing external mirror was the concave 3.0 m unit lacking the centrally drilled hole. To facilitate aligning the cavity, an intense well-collimated beam from a commercial helium-neon laser was directed in through the KRS-5 output window, down the central hole of the internal mirror, and along the cavity axis to the external mirror face. Operating in a darkened room, the reflected spot from the external mirror could easily be seen impinging either upon the glass wall of the laser tube or upon the opposing internal mirror itself. It was a simple matter to adjust, by means of the micrometer type gauges, the beam so that it illuminated a spot centered about the output hole of the internal mirror. The reflection of this illumination resulted in a beam originating from the surface of the internal mirror. Placing an ordinary microscope slide into the space between the external mirror and the Brewster angle window so that it intersected the cavity axis, the original beam directly from the laser and the beam reflected from the internal mirror (when approximately aligned)

produced easily visible spots on the slide. Adjusting the internal mirror so that the spots on the slide were coincident, the cavity was sufficiently aligned to initiate oscillation. Using the thermocouple to detect relative output intensity during oscillation, final tuning adjustments were made.

In order to align the cavity for selective oscillation over extended cavity lengths the external mirror was removed, the flat mirror and the I-beam were installed as discussed in Section III-A, and the grating placed by means of an appropriate holder onto the I-beam bench. The internal mirror adjustment settings were locked and thereafter untouched, as this mirror could be assumed focused regardless of the cavity extension. Actually the alignment problem consisted of adjusting the external mirror (grating) to support a common optic axis with the fixed internal one. A grating, however, does not have a unique optic axis, but rather an infinite number corresponding to the diffraction maxima. One might then think of a plane of optic axes. Because it would be necessary to rotate the grating to selectively choose different band components for oscillation, alignment required that the internal mirror axis lie in the "plane of axes" of the grating and remain therein under grating rotation. To accomplish this the grating was aligned in the same manner as the original external mirror, employing as the reflected beam the diffraction maximum of highest intensity. If this "plane of axes" were properly orientated, then rotating the grating

about a vertical axis by means of the appropriate micrometer-type adjustment would bring adjacent maxima into alignment. This situation would be detectable by observation of the reflected maxima upon the microscope slide, which was here placed directly in front of the grating. Rotating the grating within its holder about the central normal to its face and testing in this manner, the plane was properly orientated. Because of reduced intensities of the diffraction maxima this last step was somewhat tedious, but the procedure was found to be quite effective.

Filling and exciting the discharge tube with the proper pressures and applied voltage, oscillation on a given CO_2 line could be expected when the grating was rotated about the vertical axis to the position where equation (2.43) is satisfied for the case $i = \theta$. This being the case, the angle between the cavity axis and the grating normal would be

$$\theta = \sin^{-1}\left(\frac{m\lambda}{2b}\right). \tag{3.1}$$

For the grating used, the first order maxima at 10.6 microns required that

$$\theta = \sin^{-1}\left(\frac{10.6\mu \times 75}{2mm}\right) = 23^{\circ}\,25', \tag{3.2}$$

for cavity stability. Recall that the grating was blazed at $26^{\circ}\,45'$. Exciting the plasma in the discharge tube and rotating the grating to the region of this angle, laser oscillation was observed. Let it be noted that initiating the oscillation was quite simple when the grating was

placed upon the I-beam so as to minimize the cavity length, this minimized length being just under three meters. Beginning with a cavity length of five meters or more, proper tuning of the grating became extremely critical. Aligning the grating at this length sufficiently to induce laser action was found to be a practical impossibility. To obtain oscillation over the extended distances it was necessary to focus at the minimized separation upon a strong line, and gradually slide the grating backwards while constantly tuning alignment so as to sustain maximum output intensity. In this manner the cavity was aligned for the higher separation distances.

Output intensity was found, as expected, to be highly dependent upon gas pressures. However, it was true that with a total pressure in the neighborhood of a few torr and cavity lengths under three meters, almost any reasonable mixture of nitrogen and carbon dioxide would sustain laser oscillation. It was also found that laser oscillation depended strongly upon the voltage applied across the tube, and hence upon tube currents. For a given mixture, output intensity tended to increase with increasing applied voltages up to a point at which it maximized. Beyond this point intensity dropped off rapidly, soon becoming zero. Equal partial pressures of nitrogen and carbon dioxide resulting in a total pressure reading of five to six torr, it was found by a process of trial and error, effected a reasonably high intensity output. In this pressure range at normal operating

temperatures a typical set of values for the applied voltage and ac current through the tube was 7000 volts and 3 milliamps respectively. It follows from these values that the power input to the tube was in the neighborhood of 20 watts.

C. Operation Parameters

Some of the early investigations of the laser and its properties involved observing the output by means of the Perkin-Elmer 16U spectrograph when the cavity length amounted to just under two meters. It was soon discovered that due to longitudinal instability of the mirror positions, as discussed in Section III-A, a given band component would drift into and out of oscillation over short time intervals -- on the order of a few seconds. Calculating the Doppler width of a 10.6 micron line at the assumed temperature of 400°K, equation (2.20) yields

$$\Delta\nu_D = 52\,\text{Mhz}. \tag{3.3}$$

For the two meter cavity length the mode spacing obtained from equation (2.40) is

$$\Delta\nu_R = \frac{c}{2d} = 75\,\text{Mhz}. \tag{3.4}$$

It follows from the pertinent discussion in Section II-D that the intensity drift is accounted for by the somewhat larger value of mode spacing (3.4) in relation to Doppler width (3.3). For a longer cavity

the mode spacing decreases. For example, given d equal four meters equation (2.40) yields

$$\Delta\nu_R = \frac{c}{2d} = 38 \text{ Mhz} \quad . \tag{3.5}$$

Comparing the value of (3.5) and (3.3) and again referring to the discussion of II-D one might still expect intensity drift, but at a much reduced level. Indeed, further experiment held this to be true. Stability was found to increase with cavity length and some degree of oscillation could always be maintained, although perhaps with wide intensity variations, for cavity lengths above a minimum figure of about 2.6 m. Stability to a reasonable degree is necessary for component determination through absorption studies, hence the longer cavities were desirable for band component determination.

The main criterion in choosing cavity lengths for the selective oscillation process is angular dispersion. The displacements at the internal mirror between band component beams must be large enough to prevent more than one of the components from oscillating at the same time. In order to obtain a reasonable estimate of the necessary cavity length, let a minimum displacement of one half centimeter be assumed arbitrarily. Selecting values ν equal 960 cm^{-1}, $\Delta\nu$ equal 1.5 cm^{-1} and Θ equal $23^{\circ}25'$, equation (2.45) rearranged gives the cavity length estimate:

$$d = \frac{\Delta x_b \cos\Theta}{\Delta\nu/\nu^2} \approx 3.1 \text{ m} \quad . \tag{3.6}$$

Experiments analyzing output spectra with the Perkin-Elmer 16U spectrograph showed single line oscillation with a cavity length of 3.5 m or greater. At a distance of 2.8 m intensity peaks corresponding to grating alignment for certain band components were clearly visible in the output spectrum, which was obtained by rotating the grating at constant angular velocity and using the thermocouple for detection. However, at this cavity length intensity instability was quite high and multiple line oscillation existed.

In the next section pertinent data from output studies will be exhibited. Two of the cavity configurations used in these studies had lengths of 4 and 5.3 meters respectively. The spot sizes at the grating for these cavities, both having employed the 11.5 meter radius of curvature internal mirror, are calculated from equation (2.39). Assuming λ equal to 10.6 microns the results of these calculations are:

$$\text{for } d = 4\text{m}, \; w_o = 4.3 \text{ mm}, \tag{3.7}$$

$$\text{for } d = 5.3\text{m}, \; w_o = 4.4 \text{ mm}.$$

The spot sizes which existed at the internal mirror may be calculated using the results in (3.7) and equation (2.37). Performing this calculation one obtains:

$$\text{for } d = 4\text{m}, \; w(s = 4\text{m}) = 5.4 \text{ mm}, \tag{3.8}$$

$$\text{for } d = 5.3\text{m}, \; w(s = 5.3\text{m}) = 6.0 \text{ mm}.$$

Spot size refers to the radius and to obtain the diameter of the spot these values must be doubled. It should be recalled that these spot sizes refer to a gaussian field intensity distribution such as is present in the uniphase mode. That the laser probably operated predominantly in the uniphase mode is apparent from the relative sizes of the beam diameters, 10.8 and 12.0 mm, and the maximum diameter of the optical path down the tube, 12 mm. The discharge tube and the limitation of the exposed mirror face interfered with the beam propagation for these cavity configurations, and imposed sizable energy losses upon the system. The uniphase mode, having the largest percentage of beam energy confined within the spot diameter, enjoyed the smallest percentage loss and thus probably operated preferentially. The apparatus for the experiment should have been designed to incorporate a larger diameter discharge tube. The selection of the tube was based on work done with a preliminary laser employing the same diameter tube, work which did not involve these larger spot sizes. A certain lack of foresight must be admitted, but fortunately significant results were still obtainable with the somewhat unsatisfactory tube.

Knowing the spot sizes at the grating, one can calculate by means of equation (2.46) a reasonable estimate of the resolving powers characteristic of the cavity configurations. This is done by multiplying the number of lines per unit distance of the grating times the spot

diameter, and substituting the result into (2.46) for N. That is

$$\text{Resolving Power} = 2mw_o h, \tag{3.9}$$

where h is the number of lines per unit distance on the grating. The reason the results of (3.9) may be considered only estimates of the theoretical resolving power is that relation (2.46) was obtained assuming a constant intensity distribution as opposed to the gaussian distribution of the uniphase mode, and the arbitrary spot diameter designation of the incident beam does not conform to physically discrete boundaries. Calculating the theoretical resolving powers in the first order from (3.9) for the values given in (3.7), and multiplying the result by the factor .78 given by the grating manufacturer one obtains

$$\text{for } w_o = 4.3 \text{ mm}, \quad \text{Resolving Power} = 500, \tag{3.10}$$

$$\text{for } w_o = 4.4 \text{ mm}, \quad \text{Resolving Power} = 510.$$

Equation (2.46) shows that for a component spacing of 1.5 cm^{-1} at 960 cm^{-1}, the resolving power necessary to just resolve the two lines is

$$\frac{\lambda}{\Delta\lambda} = \frac{\nu}{\Delta\nu} = 640 \tag{3.11}$$

Equations (3.10) and (3.11) would seemingly indicate that the resolving power peculiar to the discussed cavity configurations are not or at best are barely sufficient to resolve the components of the CO_2 band. Referring to the following section (III-D) it can be seen that the system

resolved the components quite well, the lines becoming more distinct with increasing cavity length. This apparent inconsistency between theory and experiment is explained by the gain properties of the laser in conjunction with the discussion following equation (2.46).

D. Results

Output spectra were observed from the $00^{o}1\text{-}10^{o}0$ and $00^{o}1\text{-}02^{o}0$ bands of CO_2 under both selective and non-selective oscillation of the laser. All observations and studies were made on the former band and results given here shall refer to it alone, although similar results could be expected from the latter. Exciting the laser with a non-selective cavity formed by the two concave mirrors, each having radius of curvature equal to three meters and spaced at about a two meter distance, multiline oscillation was exhibited. Specifically, the output spectrum contained six lines of the P-branch having lower state J values ranging from fourteen to twenty-four, even J values only being present as predicted by selection rules. Figure five is a reproduction of this output spectrum as recorded by the Perkin-Elmer 16U spectrograph. The component showing highest intensity and thus highest optical gain is the P (22) line, having upper state value J equal twenty-one. The gain curves of figure two indicate that maximum gain is to be expected on this particular line when the population inversion ratio between the laser states has the value 1.1.

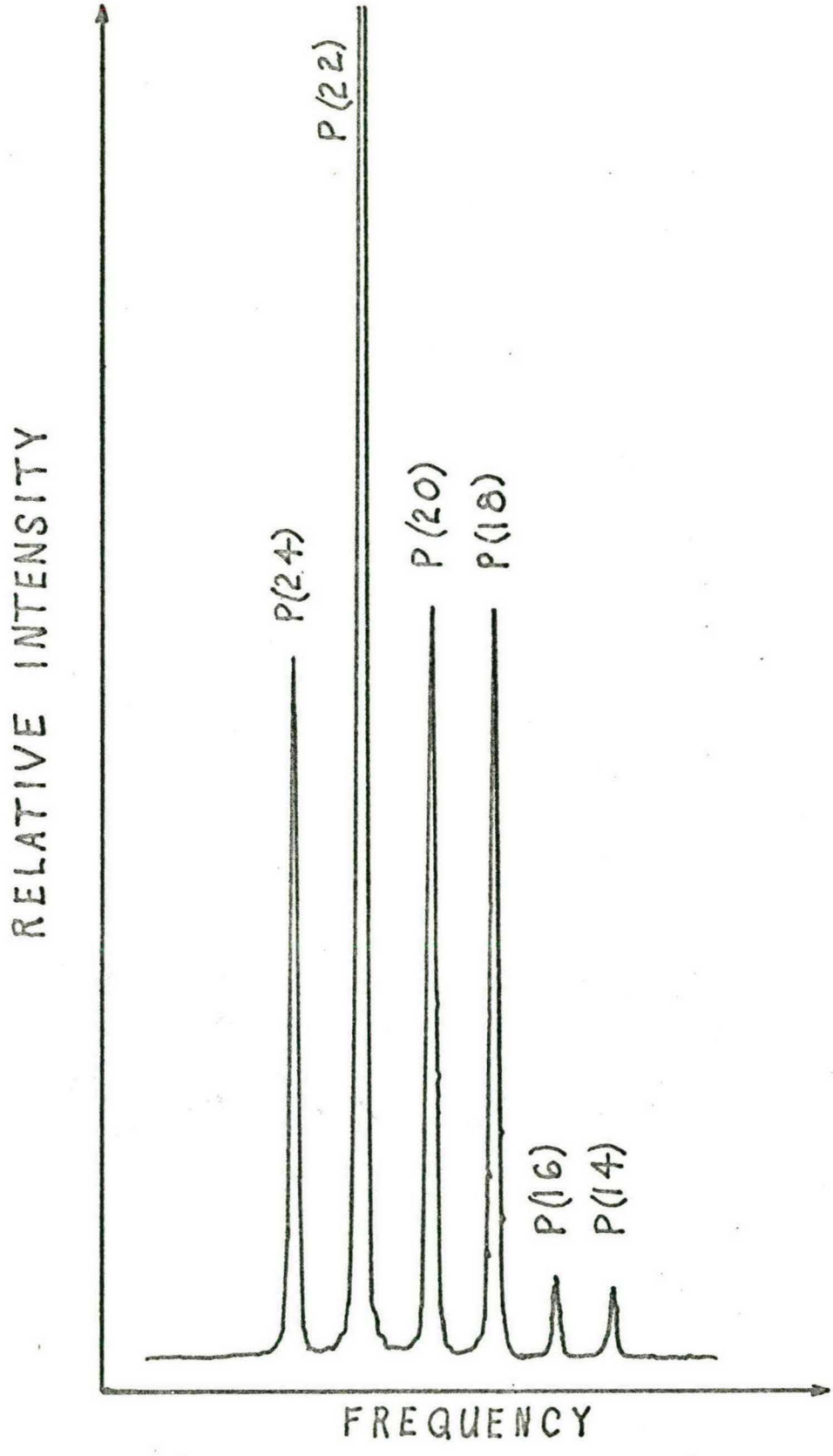

FIG. 5: Output Spectrum of the Non-Selective Cavity

Figures six through nine exhibit output spectra obtained from the laser by means of selective oscillation. They contain the general form of the band, being constituted each by both the P and R branches. The figures are reproductions of potentiometer graphs resulting from impulses received by the thermocouple used as a detector. The cavity was formed by the large radius of curvature concave mirror opposed by the diffraction grating. The grating was rotated at constant angular velocity by an electric motor, as described in the apparatus section, through the region wherein the cavity would be aligned for oscillation over the band. As the cavity focused successively for each component of the band, those capable of oscillation stimulated the thermocouple through the derived output with resulting peaks recorded graphically. The graphs of figure six and seven were taken with a laser cavity spacing of 4 meters, figures eight and nine with a spacing of 5.3 meters. At these distances the output was relatively stable and the lines clearly resolved. Comparing figures six and eight, one sees that the lines are more distinctly resolved at the larger cavity length, but that the number of lines capable of oscillation is much higher at the shorter length. Actually, in order to obtain the number of lines present in figure eight the laser was operated at below equilibrium temperature, in a transient heating state. Gain increases with decreased temperatures, as implied by equations (2.31) and (2.32). Operating at equilibrium temperatures with the longer 5.3 meter

Figures 6, 7, 8, 9.

These four figures exhibit the recorded output spectra of the laser, obtained through selective oscillation. The cavities were formed in all cases by the 11.5 m radius of curvature concave internal mirror opposed by the grating. The spectra in figures 6 and 7 were recorded when the cavity length was 4 m, those in figures 8 and 9 when the cavity length was 5.3 m. Figures 7 and 9 show absorption effects from an NH_3 cell which was placed in the output beam between the laser and the detecting thermocouple. Most significant is the complete absorption of the R(14) line.

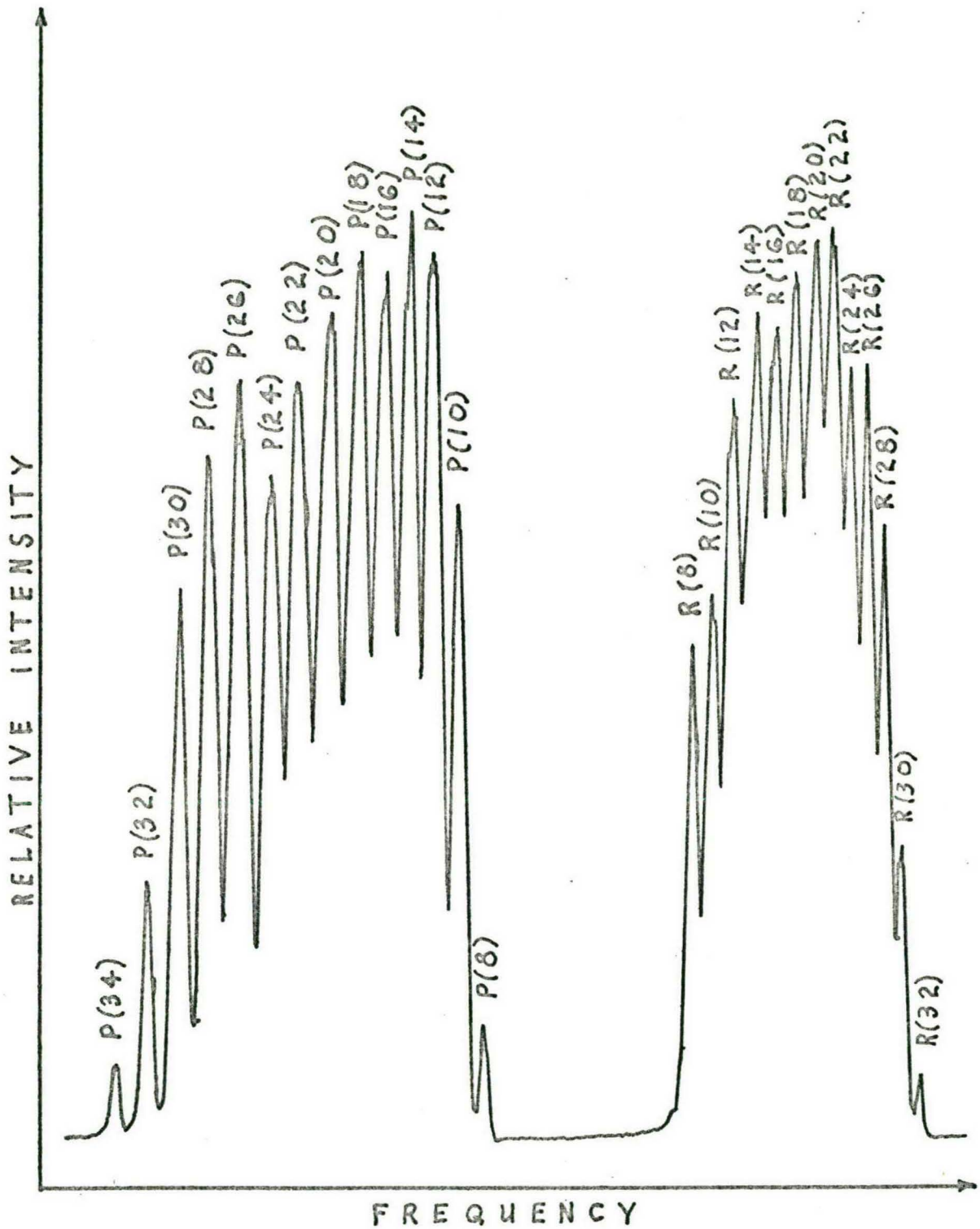
RELATIVE INTENSITY
FREQUENCY
P(34)
P(32)
P(30)
P(28)
P(26)
P(24)
P(22)
P(20)
P(18)
P(16)
P(14)
P(12)
P(10)
P(8)
R(8)
R(10)
R(12)
R(14)
R(16)
R(18)
R(20)
R(22)
R(24)
R(26)
R(28)
R(30)
R(32)

FIGURE 6

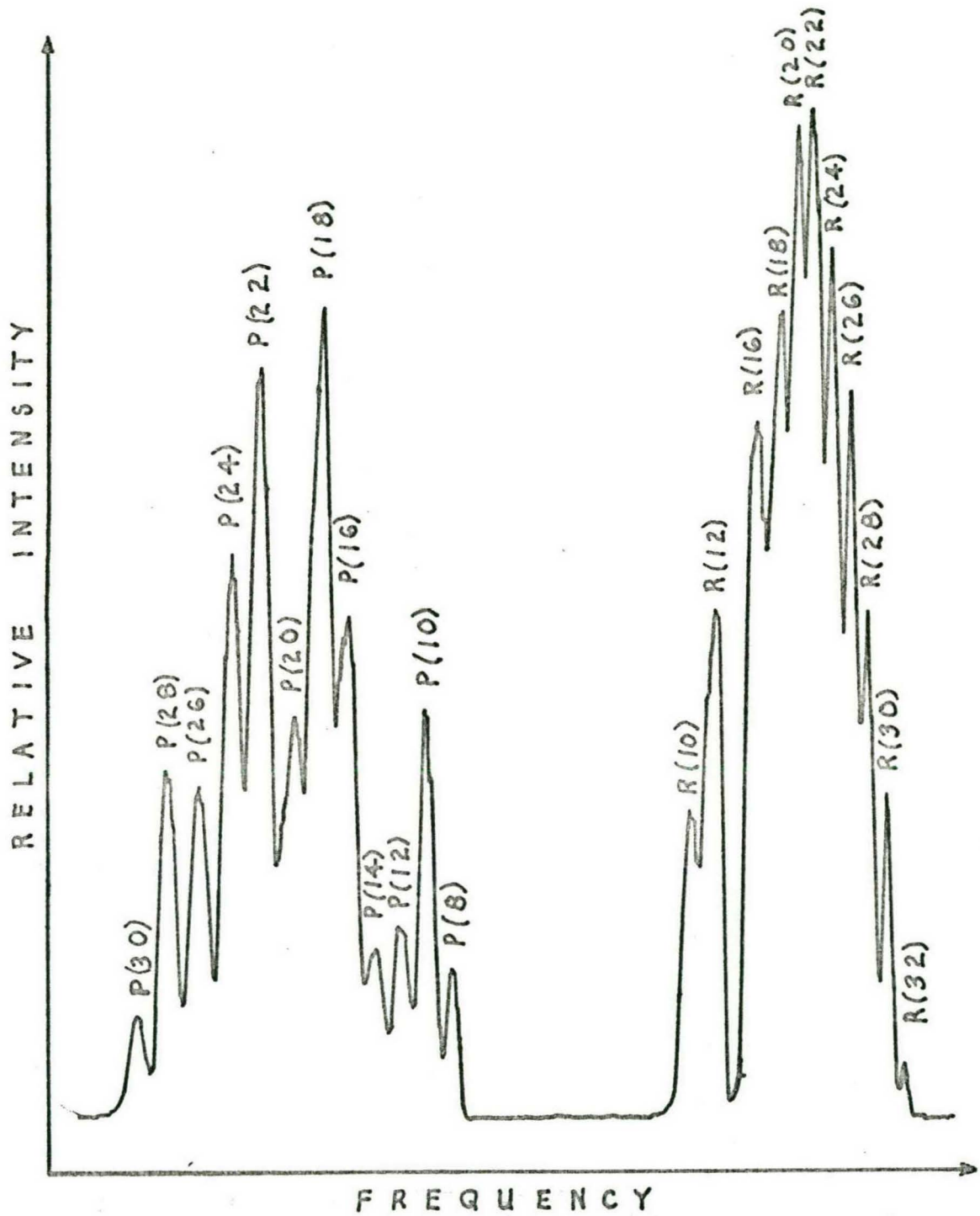
RELATIVE INTENSITY
FREQUENCY
P(30)
P(28)
P(26)
P(24)
P(22)
P(20)
P(18)
P(16)
P(14)
P(12)
P(10)
P(8)
R(10)
R(12)
R(16)
R(18)
R(20)
R(22)
R(24)
R(26)
R(28)
R(30)
R(32)

FIGURE 7

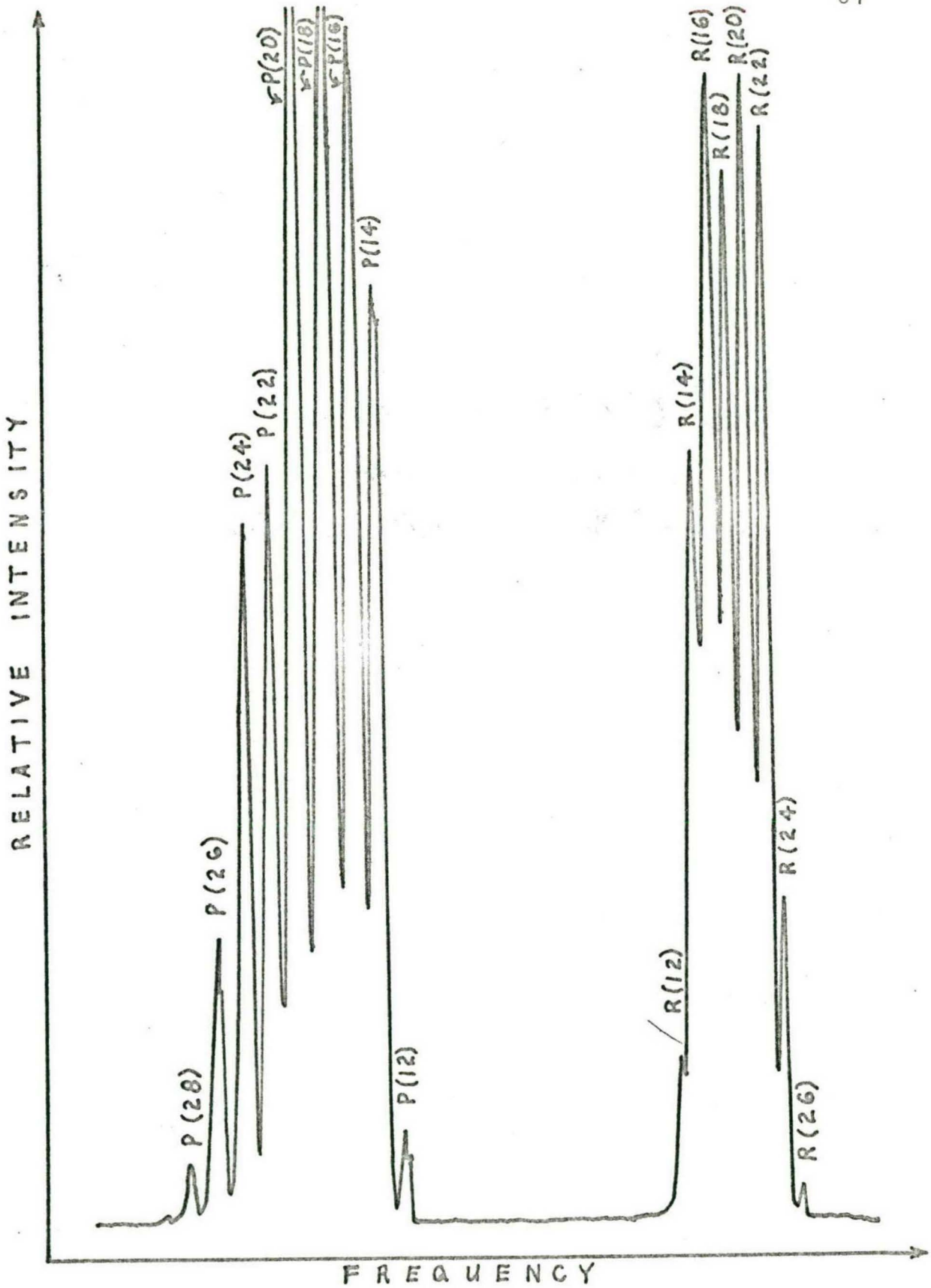
RELATIVE INTENSITY
FREQUENCY
P(28)
P(26)
P(24)
P(22)
P(20)
P(18)
P(16)
P(14)
P(12)
R(12)
R(14)
R(16)
R(18)
R(20)
R(22)
R(24)
R(26)

FIGURE 8

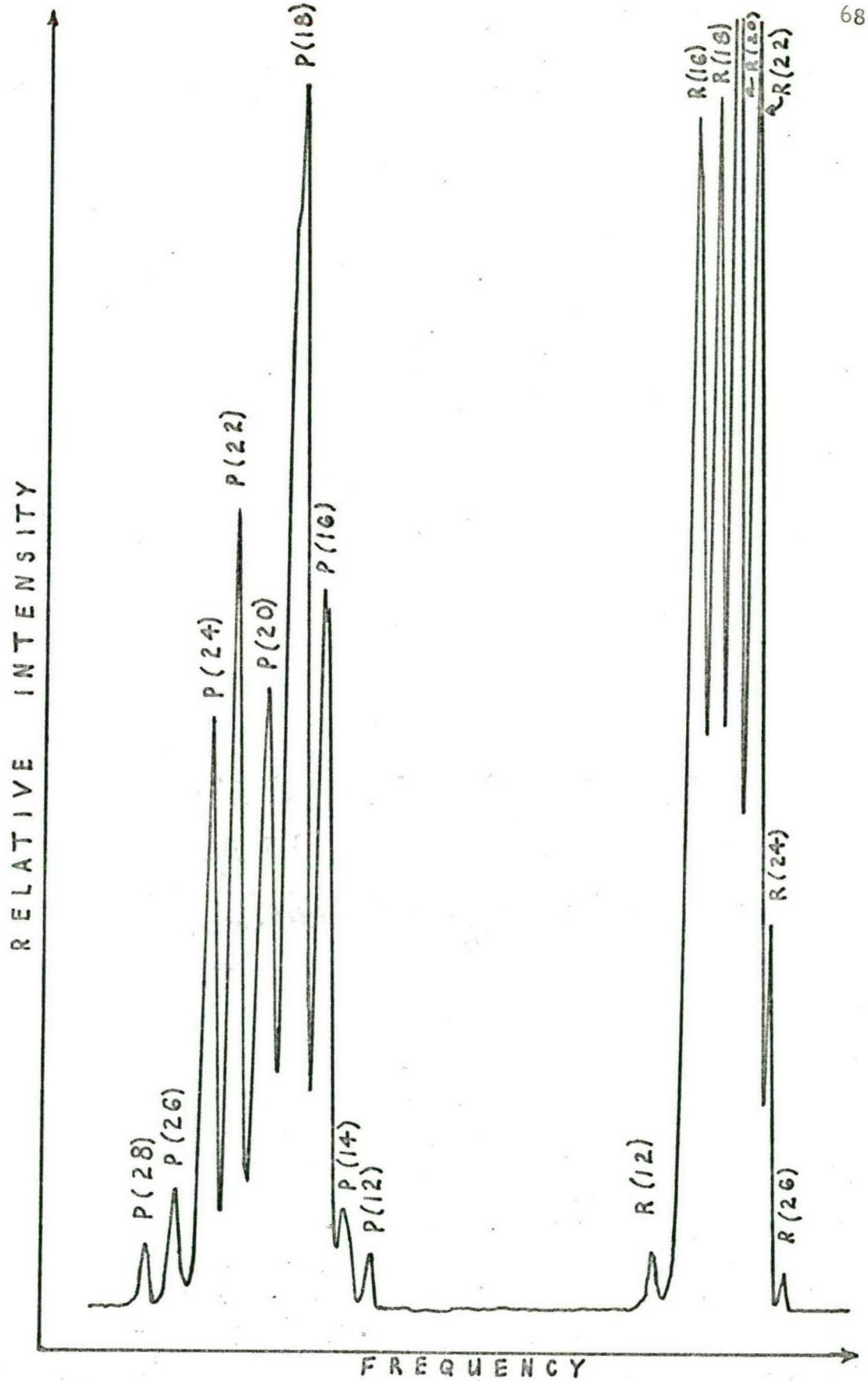
RELATIVE INTENSITY
FREQUENCY
P(28)
P(26)
P(24)
P(22)
P(20)
P(18)
P(16)
P(14)
P(12)
R(12)
R(16)
R(18)
R(20)
R(22)
R(24)
R(26)

FIGURE 9

cavity as was done with the 4 meter cavity length, only four lines were seen, two in each branch. This rapid drop off in the number of lines observed is attributed to increasing spot sizes imposing loss upon the system through confliction with cross-sectional cavity dimensions.

Figures seven and nine are graphs taken from runs under circumstances duplicate respectively to those under which six and eight were taken, but with the insertion of the absorption cell containing one fifth of an atmosphere of ammonia gas into the output beam between the output window and the thermocouple detector. Knowing the positions of the CO_2 band components (35) and those absorption lines of NH_3 in the region of the band (36), comparison of the figures six and eight with seven and nine respectively enabled determination of the band components by branch and angular momentum quantum number J.

Table two contains a listing of the observed band components, the pertinent NH_3 absorption lines, and the estimated relative degree to which these lines were absorbed as indicated in figures six through nine. Wavenumber values contained in this table are taken from references (35) and (36).

TABLE 2

CO_2 Line	λ_{CO_2} (cm^{-1})	Significant λ_{NH_3} (cm^{-1})	Relative Absorption 5.3 m Cavity	Relative Absorption 4.0 m Cavity
P(34)	931.00	*		total
P(32)	932.96	*		total
P(30)	934.89	934.3		high
P(28)	936.80	935.89	weak	medium
P(26)	938.68	937.6	medium	medium
P(24)	940.54		weak	weak
P(22)	942.38		none	none
P(20)	944.19		medium	medium
P(18)	945.98		none	none
P(16)	947.74	948.25	medium	medium
P(14)	949.48	949.35	high	high
P(12)	951.19	951.8	weak	high
P(10)	952.88			weak
P(8)	954.54	957.85		none
R(8)	967.70	967.35		total
R(10)	969.14			weak
R(12)	970.54		medium	weak
R(14)	971.93	971.9	total	total
R(16)	973.28		weak	weak
R(18)	974.62		weak	weak
R(20)	975.93		weak	none
R(22)	977.21		weak	none
R(24)	978.47		none	none
R(26)	979.70		none	weak
R(28)	980.91			weak
R(30)	982.09			none
R(32)	983.25	991.7		none

*Strong absorption lines of unspecified wavelength are present in this region.

IV. CONCLUSIONS

A CO_2 laser has been designed, constructed, and operated selectively over various band components. Oscillation has been observed upon twenty-seven transitions in both the P and R branches of the $00^{\circ}1-10^{\circ}0$ band, the majority of these being unobtainable in the conventional non-selective laser. The optical gain peculiar to the individual transitions has been calculated theoretically, based upon specific assumptions and approximations, and found to explain satisfactorily the results of experiments. The selective oscillation mechanism has been shown an effective method for producing and regulating laser output, and one may conjecture important applications of this mechanism in future experimental and practical endeavors. Stability of output intensity was found to increase with laser cavity extension, although at the cost of inducing longitudinal multimode oscillation.

Interesting extensions of the present work might include further experimental investigations of gain dependencies, stability factors, and methods of raising Q values of the selective cavity.

REFERENCES

1. A. Einstein, "Zur Quanten Theorie der Strahlung," Physik Zeitschrift 18, 121 (1917).

2. B. A. Lengyel, Introduction to Laser Physics (Wiley and Sons, New York, 1966).

3. A. L. Schawlow and C. H. Townes, "Infrared and Optical Masers," Physical Review 112, 1940 (1958).

4. T. H. Maiman, "Stimulated Optical Radiation on Ruby Masers," Nature 187, 493 (1960).

5. A. Javan, W. R. Bennett, and D. R. Herriott, "Population Inversion and Continuous Optical Maser Oscillation in a Gas Discharge Containing a He-Ne Mixture," Physical Review Letters 6, 106 (1961).

6. W. V. Smith and P. P. Sorokin, The Laser (McGraw-Hill, Inc., New York, 1966).

7. C. K. N. Patel, "Continuous-Wave Laser Action on Vibrational-Rotational Transitions of CO_2," Physical Review 136, A1187 (1964).

8. C. K. N. Patel, "CW High Power N_2CO_2 Laser," Applied Physics Letters 7, 15 (1965).

9. G. Moeller and J. D. Rigden, "Observation of Laser Action in the R-Branch of CO_2 and N_2O Vibrational Spectra," Applied Physics Letters 8, 69 (1966).

10. G. Herzberg, Infrared and Raman Spectra of Polyatomic Molecules (D. Van Norstrand Inc., New York, 1945).

11. C. K. N. Patel, "Vibration Energy Transfer - An Efficient Means of Selective Excitation in Molecules," Physics of Quantum Electronics (McGraw-Hill, New York, 1966).

12. K. Dressler, Journal of Chemical Physics 30, 1921 (1959).

13. N. N. Sobolev and V. V. Sokovikov, "A Mechanism Ensuring Level Population Inversion in CO_2 Lasers," JETP Letters 4, 204 (1966).

14. T. L. Cottrell and J. C. McCoubrey, Molecular Energy Transfer in Gases (Butterworth, London, 1961).

15. J. E. Morgan and H. I. Schiff, Canadian Journal of Chemistry 41, 903 (1963).

16. V. N. Kondratyev, Chemical Kinetics of Gas Relations (Addison-Wesley, Reading, Mass., 1964).

17. H. Statz, C. L. Tang, G. F. Koster, "Transition Probabilities between Laser States in Carbon Dioxide," Journal of Applied Physics 37, 4278 (1966).

18. E. V. Condon and G. H. Shortley, The Theory of Atomic Spectra (Cambridge University Press, Cambridge, England, 1957).

19. A. R. Edmonds, Angular Momentum in Quantum Mechanics (Princeton University Press, Princeton, N. J., 1957).

20. T. Holstein, Physical Review 72, 1212 (1947).

21. C. K. N. Patel, "Selective Excitation Through Vibrational Energy Transfer and Optical Maser Action in N_2-CO_2," Physical Review Letters 13, 617 (1964).

22. C. K. N. Patel, P. K. Tien and J. H. McFee, "CW High-Power CO_2-N_2-He Laser," Applied Physics Letters 7, 290 (1965).

23. C. K. N. Patel, "Interpretation of CO_2 Optical Maser Experiments," Physical Review Letters 12, 588 (1964).

24. A. C. G. Mitchell and M. W. Zemansky, Resonance Radiation and Excited Atoms (Cambridge University Press, New York, 1934).

25. K. F. Herzfeld and T. A. Litovitz, Absorption and Dispersion of Ultrasonic Waves (Academic Press, New York, 1959).

26. G. T. di Francia, "Theory of Optical Resonators," Proceedings of the International School of Physics - Enrico Fermi, Course XXXI (Academic Press, New York, 1964).

27. H. Kogelnik and T. Li, "Laser Beams and Resonators," Applied Optics 5, 1550 (1966).

28. G. D. Boyd and H. Kogelnik, "Generalized Confocal Resonator Theory," Bell Systems Technical Journal 41, 1347 (1962).

29. A. G. Fox and T. Li, "Resonant Modes in a Laser Interferometer," Bell Systems Technical Journal 40, 453 (1961).

30. G. D. Boyd and J. P. Gordon, "Confocal Multimode Resonator for Millimeter through Optical Wavelength Masers," Bell Systems Technical Journal 40, 489 (1961).

31. W. W. Rigrod, Applied Physics Letters 2, 51 (1963).

32. F. A. Jenkins and H. E. White, Fundamentals of Optics (McGraw-Hill Inc., New York, 1957).

33. D. R. Corson and P. Lorrain, Introduction to Electromagnetic Fields and Waves (W. H. Freeman and Co., San Francisco, 1962).

34. J. A. Anderson and R. W. Porter, "Ronchi's Method of Optical Testing," Astrophysical Journal, 264 (1929).

35. These unpublished wavenumber values for the $00^{o}1$-$10^{o}0$ band components of CO_2 are taken from results of calculations based upon B values determined experimentally through combination relations. The experiments were done at "The Ohio State University" under the direction of Dr. K. N. Rao, and the calculations were performed by Mr. R. Oberly.

36. International Union of Pure and Applied Chemistry Commission on Molecular Structure and Spectroscopy, Table of Provisional Wavenumber Standards - Part IV, Chart 31.